AD-A201 451

ORT DOCUMENTATION PAGE

Form Approved
OMB No. 0704-0188

1a. REPORT SECURITY CLASSIFICATION UNCLASSIFIED	1b. RESTRICTIVE MARKINGS
2a. SECURITY CLASSIFICATION AU[illegible]	3. DISTRIBUTION / AVAILABILITY OF REPORT Approved for public release; distribution unlimited.
2b. DECLASSIFICATION / DOWNGRA[illegible] SCHEDULE	
4. PERFORMING ORGANIZATION [illegible] NUMBER(S) N00014-85-C-0141-AR8	5. MONITORING ORGANIZATION REPORT NUMBER(S)
6a. NAME OF PERFORMING ORGANIZATION Washington State University	6b. OFFICE SYMBOL (If applicable)
6c. ADDRESS (City, State, and ZIP Code) Department of Physics Washington State University Pullman, WA 99164-2814	7a. NAME OF MONITORING ORGANIZATION Office of Naval Research
	7b. ADDRESS (City, State, and ZIP Code) Physics Division, Code 1112 Arlington, VA 22217-5000
8a. NAME OF FUNDING / SPONSORING ORGANIZATION	8b. OFFICE SYMBOL (If applicable)
8c. ADDRESS (City, State, and ZIP Code)	9. PROCUREMENT INSTRUMENT IDENTIFICATION NUMBER N00014-85-C-0141
	10. SOURCE OF FUNDING NUMBERS

PROGRAM ELEMENT NO	PROJECT NO.	TASK NO	WORK UNIT ACCESSION NO
61153N	4126934		

11. TITLE (Include Security Classification)
Research on Acoustical Scattering, Diffraction Catastrophes, Optics of Bubbles, and Acoustical Phase Conjugation

12. PERSONAL AUTHOR(S)
Marston, P. L.

13a. TYPE OF REPORT	13b. TIME COVERED	14. DATE OF REPORT (Year, Month, Day)	15. PAGE COUNT
Annual Summary	FROM 870916 TO 881015	881031	52

16. SUPPLEMENTARY NOTATION
The telephone number for the Principal Investigator, P. L. Marston, is (509) 335-5343 or 335-9531

17 COSATI CODES			18. SUBJECT TERMS (Continue on reverse if necessary and identify by block number)
FIELD	GROUP	SUB-GROUP	Acoustical Scattering, Lamb Waves, Resonances, Diffraction Catastrophes, Caustics, Light Scattering, Microbubbles, Bubbles, Phase Conjugation (Acoustical).
20	01		
20	06		

19. ABSTRACT (Continue on reverse if necessary and identify by block number)

The research summarized concerns several aspects of the propagation and scattering of acoustical and optical waves. The topics discussed fall under the following four categories:

(A) A generalization of the geometrical theory of diffraction which describes surface-guided wave contributions to the scattering of sound from smooth elastic objects in water; the effect of curvature on Lamb wave velocities on thick shells; a product expansion of the S function for elastic spheres;

20. DISTRIBUTION / AVAILABILITY OF ABSTRACT	21. ABSTRACT SECURITY CLASSIFICATION
☒ UNCLASSIFIED/UNLIMITED ☐ SAME AS RPT ☐ DTIC USERS	UNCLASSIFIED

22a. NAME OF RESPONSIBLE INDIVIDUAL	22b. TELEPHONE (Include Area Code)	22c. OFFICE SYMBOL
L. E. Hargrove, ONR Physics Division	(209) 696-4221	ONR Code 1112

DD Form 1473, JUN 86 — Previous editions are obsolete. — SECURITY CLASSIFICATION OF THIS PAGE

UNCLASSIFIED

19. ABSTRACT (continued)

B. Acoustical and optical caustics and associated wavefields: unfolding axial caustics; observations of lips caustics in light backscattered from oblate drops; and observations of acoustical and optical transverse cusps produced by reflection.

C. Physical optics of bubbles in water: observations of Brewster angle light scattering; observations of backscattering from rising bubbles; asymptotic series for critical angle scattering useful for determining bubble sizes; and

D. Acoustic phase conjugation and aspects of wavefront reversal: a theory for wavefront reversal via three-wave mixing in a layer of enhanced nonlinearity as caused, for example, by a layer of microbubbles in water; the present status of experiments on three-wave mixing; and the possibility of phase conjugation via reflection from curved vibrating surfaces.

REPORT NUMBER N00014-85-C-0141-AR8

DEPARTMENT OF PHYSICS
WASHINGTON STATE UNIVERSITY
PULLMAN, WA 99164-2814

ANNUAL SUMMARY REPORT

OCTOBER, 1988

Title:

Research on Acoustical Scattering, Diffraction Catastrophes, Optics of Bubbles, and Acoustical Phase Conjugation

by

Philip L. Marston

Prepared for:
OFFICE OF NAVAL RESEARCH
PHYSICS DIVISION—CODE 1112
CONTRACT NO. N00014-85-C-0141

ABSTRACT

The research summarized concerns several aspects of the propagation and scattering of acoustical and optical waves. The topics discussed fall under the following four categories:

A. A generalization of the geometrical theory of diffraction which describes surface-guided wave contributions to the scattering of sound from smooth elastic objects in water; the effect of curvature on Lamb wave velocities on thick shells; a product expansion of the S function for elastic spheres.

B. Acoustical and optical caustics and associated wavefields: unfolding axial caustics; observations of lips caustics in light backscattered from oblate drops; and observations of acoustical and optical transverse cusps produced by reflection.

C. Physical optics of bubbles in water: observations of Brewster angle light scattering; observations of backscattering from rising bubbles; asymptotic series for critical angle scattering useful for determining bubble sizes.

D. Acoustic phase conjugation and aspects of wavefront reversal: a theory for wavefront reversal via three-wave mixing in a layer of enhanced nonlinearity as caused, for example, by a layer of microbubbles in water; the present status of experiments on three-wave mixing; and the possibility of phase conjugation via reflection from curved vibrating surfaces.

TABLE OF CONTENTS

I. SCATTERING OF SOUND FROM ELASTIC OBJECTS IN WATER

A. Project to Extend GTD to Smooth Elastic Objects

The extension of the geometrical theory of diffraction (GTD) to backscattering from elastic objects in water should allow complicated scattering problems to be partitioned into geometry and the determination of local guided-wave/acoustic-field interactions from continuum mechanics. It gives a simple and quantitative understanding of the scattering process which could be useful both for inverse problems and for predicting how changes in an object will affect the scattering. Heuristic support for the basic ideas were put forth by Soviet researchers.[1] In their approach, however, the coefficient which describes the coupling of surface-guided waves with the acoustic field was determined by a fitting procedure. Independently, and at about the same time, a rigorous analysis of backscattering from elastic spheres was carried out by Williams and Marston[2,3] based on the Watson transformation. That analysis gave an exact expression for the required complex coupling coefficient G_l for the specific case of a solid elastic sphere. In that expression, however, the dependence of G_l on physically relevant parameters was obscured by the complexity of the expression.

A desirable form for G_l is one in which it manifests its dependence on the properties of the surface wave on the object. These properties are the local phase velocity c_l and the radiation damping parameter β_l. Such relationships were obtained for $|G_l|$ in the preceding contract year with the following result for the sphere and circular cylinder cases, respectively[4,5]

$$|G_l^{sp}| \approx 8\pi\beta_l c/c_l, \quad |G_l^{cy}| \approx 8\pi\beta_l/(\pi x)^{1/2}, \tag{1,2}$$

where $x = ka$, a is the radius of the object and $k = 2\pi/\lambda$ where λ and c are the wavelength and sound speed in water. These expressions were confirmed with the exact result for solid spheres and Veksler's fitted result for Lamb waves on a hollow cylinder.[4,5]

B. Approach and Accomplishments on Extending GTD

One unresolved issue was the phase of the complex coefficient G_l for the various cases of interest. These were calculated for certain special cases, as described below, by a tedious extension of the method used in the derivation of Eqs. (1) and (2). The approach is based on the observation that the Fabry-Perot/GTD representation of the form function should reduce to the result of the Breit-Wigner form of resonance scattering theory (RST) with an appropriate background for the special case of small β_l where the Breit-Wigner form should be applicable. While the resulting approximations for $|G_l|$, Eqs. (1) and (2), do not depend on the choice of the background, the resulting approximations for the phase do. The results[6] are summarized below where the superscripts r and s designate the rigid and soft background choices, respectively

$$\arg(G_l^{sp})^r \approx 0 \quad , \qquad \arg(G_l^{sp})^s \approx \pi, \tag{3,4}$$

$$\arg(G_l^{cy})^s \approx \pi/4, \qquad \arg(G_l^{cy})^s \approx 5\pi/4 \, . \tag{5,6}$$

where sp denotes sphere and cy denotes circular cylinder. Equations (3) and (5) should be applicable to solid scatterers which are sufficiently dense that RST with a rigid background choice is a good approximation to the exact scattering. Equations (4) and (6) may only be applicable to very thin shells for which a soft background causes RST to be a useful approximation.

The correctness of the above analysis was confirmed in one case by comparison with exact results from a partial-wave series (PWS), Fig. 1. The GTD-based synthesis shown uses the approximation $f \approx f_S + f_{l=R} + f_{l=WG1}$ where

$$f_l = \frac{-G_l e^{-2(\pi-\theta_l)\beta_l} e^{i\eta_l}}{\left[1 + j \exp(-2\pi\beta_l + i2\pi xc/c_l)\right]}, \; G_l \approx 8\pi\beta \, c/c_l \, , \; f_S \approx \left(\frac{\rho_E c_L - \rho c}{\rho_E c_L + \rho c}\right) e^{-i2ka} \tag{7a,b,8}$$

where for the present problem of spheres $j = +1$. Equation (8) is a simple approximation of the specular contribution for a solid sphere of density ρ_E, longitudinal sound speed c_L in water of density ρ. The agreement between the exact and GTD synthesis of $|f|$ in Fig. 1 is

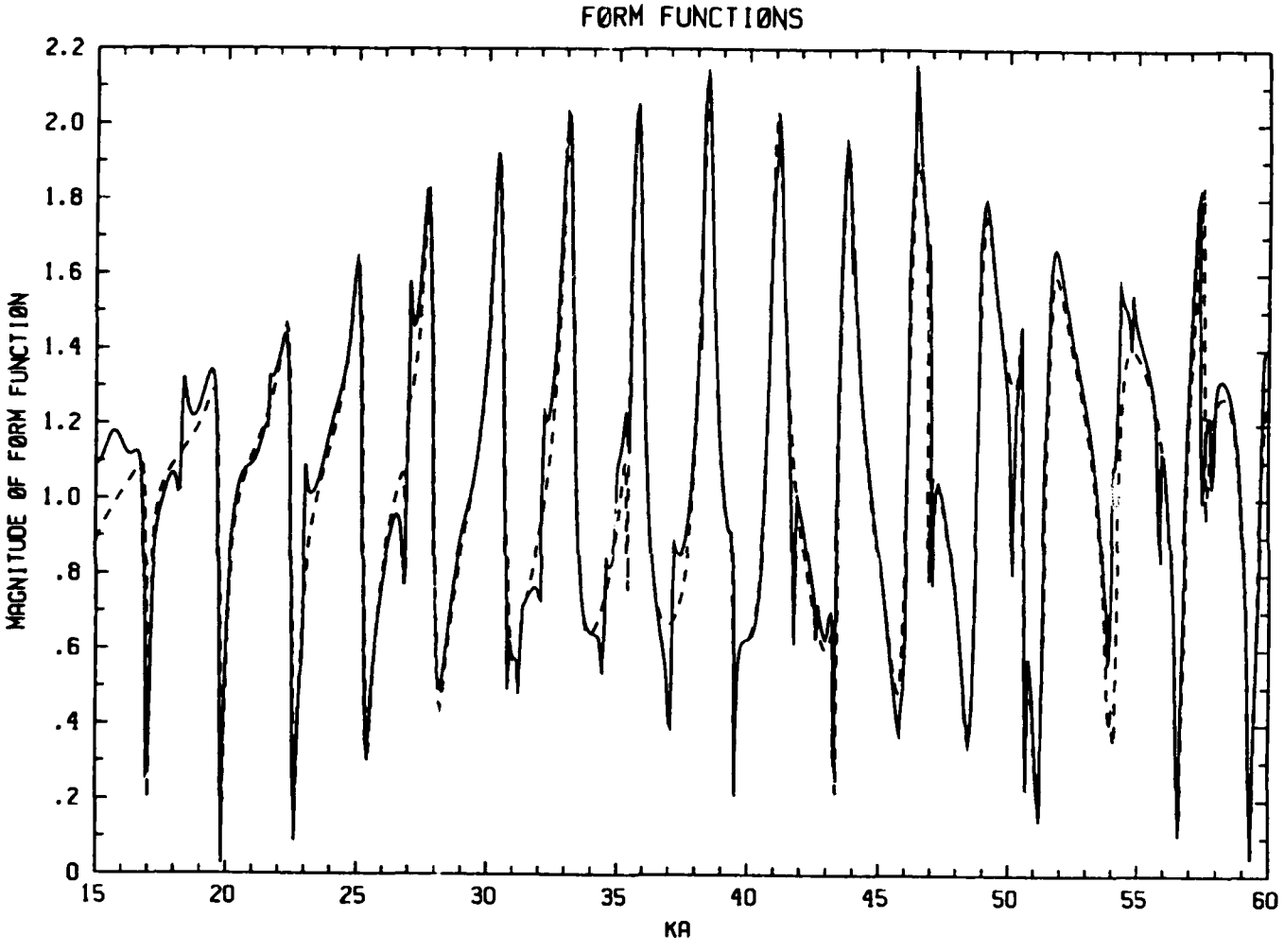

Fig. 1. The solid curve is the exact |f| from the partial wave series for backscattering from a tungsten carbide sphere in water. The dashed curve is the simple synthesis based on Eqs. (7) and (8) as described in the text. The computations were done at the Naval Coastal Systems Center in collaboration with Kevin L. Williams.

satisfactory considering only the Rayleigh wave and slowest whispering gallery wave contributions were included in the sum over l.

In a related accomplishment, an approximation was derived in a heuristic way for the contribution of a surface wave to scattering from a circular cylinder not restricted to the backward direction.[7] Furthermore, it was possible to use GTD methods to relate $\arg(G_l^{sp})$ to $\arg(G_l^{cy})$ directly, without reference to RST. It was assumed that $ka >> 1$ and β_l and c_l are the same for the sphere and for the cylinder so that the targets are either both solid or both shells. The result is $\arg(G_l^{sp}) \approx \arg(G_l^{cy}) - (\pi/4)$ which agrees with Eqs. (3) - (6). The method of comparing cylinder and sphere scattering is like that of Sec. VI of Ref. 5 except that now the phase was found.

The surface-elastic-wave/GTD approach to modeling Lamb wave contributions to backscattering from a hollow shell was confirmed in our earlier work by comparison with data.[4,8] Though there was agreement between theory and data, without the use of any adjustable parameters, it was necessary to use the Watson transform methodology to find the Lamb wave parameters c_l and β_l. It would be desirable to demonstrate that these can be found from the local continuum mechanics of a water loaded curved plate.

A simple approximation was obtained which is an advancement toward the aforementioned goal. In this approximation the effect of curvature on the phase velocity along the outer surface of a curved plate was estimated.[9] The result was compared with the results of the Watson transform for the case of a spherical stainless-steel shell having a ratio of inner to outer radius b/a of 0.838 and a = 19.05 mm. The shell thickness is h = a - b = 3.1 mm. In the discussion which follows $l = a_0$ designates the antisymmetric (i.e. flexural) Lamb wave while $l = s_0$ is the symmetric (i.e. extensional) Lamb wave. First consider the exact results from the Watson transform for c_l/c for the sphere in water. The set of curves which begin at $ka = 20$ in Fig. 2 give the predicted c_l/c with the solid curve being $l = a_0$ and the dashed curve being $l = s_0$. The curves which begin at $ka \approx 0$ and lie below the set of exact curves (described above) are given by taking $c_l = (c_l)_P$ where $(c_l)_P$

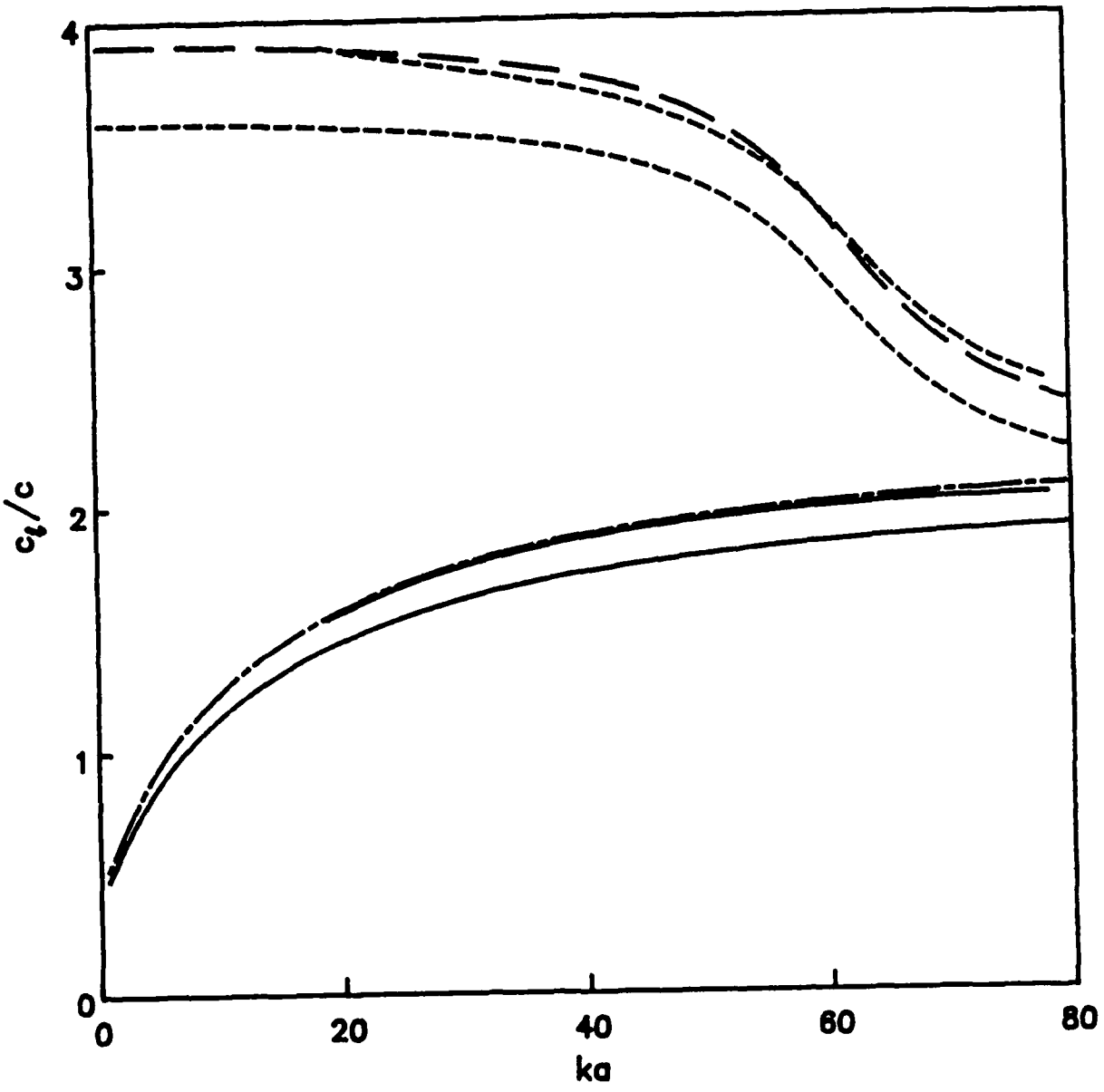

Fig. 2. The set of curves which begin at ka = 20 give the exact c_l/c according to the Watson transform for Lamb waves on a shell in water where c is the speed of sound in water. The lower of the solid and short-dashed curves use Lamb's result $(c_l)_p$ for a flat plate. The other set (which are in much better agreement with the exact theory) incorporate the curvature connection given by Eq. (9).

is the velocity of the respective wave on a *flat plate* of thickness h in vacuum as given by Lamb's original analysis. For this set, the solid curve has $l = a_o$ while the dashed curve has $l = s_o$. The curves with the alternating long-short dashes and the long dashes are a much improved approximation in which

$$c_l = (c_l)_p/[1 - (h/2a)]. \tag{9}$$

The denominator in Eq. (9) is a novel method of accounting for the curvature of the shell. The velocity of the wave at the midpoint of the shell material [where the radius is a - (h/2)] is taken to be $(c_l)_p$; this velocity is projected to the outer surface (of radius a) to give c_l. The general agreement with the exact result shows that c_l could have been obtained from *local* surface properties had we not derived the exact partial-wave series.

In related work, a GTD based phenomenological model was examined for the broad mid-frequency enhancement of backscattering from thin spherical shells. A graduate Student, Cleon Dean, participated in the computations.

C. Product Expansion of the S Function for Scattering from Elastic Spheres Having Multiple Resonances

In related work, the implicit assumptions of formal resonance scattering theory[10] have been corrected and clarified. Associated with the scattering phase shift δ_n of the nth partial wave for a sphere of radius a is the function $S_n(x) = \exp[2i\delta_n]$ where $x = ka$. A theorem from *classical* scattering theory[11] was applied by Marston to obtain the following *product expansion* which appears to be important and novel for acoustics

$$S_n = \pm e^{-2ix} \prod_l \frac{(x^*_{nl} - x)(x_{nl} + x)}{(x^*_{nl} + x)(x_{nl} - x)} \prod_j \frac{(iL_{nj} - x)}{(iL_{nj} + x)} \tag{10}$$

where the $x_{nl} \equiv X_{nl} - i(\Gamma_{nl}/2)$ lie in the fourth quadrant and $L_{nj} > 0$. Unlike a *sum* expansion (stated in some acoustic RST literature[10]) S_n remains manifestly unitary even

for multiple resonances l. This S_n may be used to split off elastic contributions to the partial-wave form function f_n for backscattering in analogy with RST. In the case of only two resonances (labeled $l = 1$ and 2)

$$f_n \approx f_n^{(b)} + f_{n1} + f_{n2} + f_n^{(int)} \tag{11}$$

where $f_n^{(b)}$ is a background term and it is assumed that $x + X_{nl} >> \Gamma_{nl}$. The f_{nl} have a Breit-Wigner form

$$f_{nl} = \exp(2i\xi_n)[(2n+1)/x](-1)^n \Gamma_{nl}[X_{nl} - x - (i/2)\Gamma_{nl}]^{-1} \tag{12}$$

and ξ_n is the phase shift associated with $f_n^{(b)}$. The *interaction term* $f_n^{(int)}$ vanishes as $\Gamma_{nl}/|x - X_{nl}| \rightarrow 0$ for $l = 1$ or 2. The implicit assumptions of RST are that S_n has the product form, Eq. (10), and not the sum expansion usually written.[10] Furthermore, the interaction term $f_n^{(int)}$ is neglected when f_n is written as a sum of Breit-Wigner terms.

The product expansion over index j in Eq. (10), manifestly corresponds to poles (or generalized resonances) for which there is no restoring force but only damping. (These poles lie on the imaginary axis at $x = -iL_{nj}$.) The physical significance of such a pole is illustrated by considering the $n = 1$ or dipole partial-wave. The L_{1j} pole(s) account for the translational motion of a movable elastic sphere.

II. ACOUSTICAL AND OPTICAL CAUSTICS AND ASSOCIATED WAVEFIELDS (DIFFRACTION CATASTROPHES)

A. Project to Explore Novel Acoustical and Optical Diffraction Catastrophes

In previous research we described examples of acoustical and optical diffraction catastrophes in certain reflection and scattering problems.[4] Since such catastrophes decorate the caustics of geometrical optics, the amplitudes of the wavefields tend to be large when the wavelength is short. Three recent accomplishments are described below.

B. Unfolding Acoustical Axial Caustics of Glory Scattering with Harmonic Angular Perturbations of Toroidal Wavefronts

This theory and an analysis of the associated acoustic wavefields were a part of the recently completed Ph.D. dissertation project of W. P. Arnott.[12,13] Attention was restricted to the simplest class of harmonic angular perturbation $f(\psi)$ of the toroidal wavefront $\tilde{W}(s)$:

$$\tilde{W}(s) = -\frac{(s-b)^2}{2\alpha}, \quad f(\psi) = \frac{\delta}{2}\left(1 + \cos p\psi\right), \tag{13,14}$$

where s and ψ are radial and angular polar coordinates, the positive constants b and α each have dimensions of length and specify the focal circle radius and position for the unperturbed wavefront while δ is the strength of the perturbation and $p = 2, 3, 4 \ldots$ describes the harmonic frequency of the perturbation. The outgoing wavefronts of interest are of the form

$$W(s,\psi) = \tilde{W}(s) - f(\psi), \tag{15}$$

which is relevant to several scattering or reflection problems for nonspherical objects.[12,13] (One example is Lamb wave contributions to backscattering from slightly oblate or prolate shells for which case $p = 2$.) Let the z axis be the extension of the axis along $s = 0$ where $W = 0$ corresponds to the plane $z = 0$. It is convenient to restrict attention to weak perturbations for which $|\beta| p^2 \lesssim 0.025$ where $\beta \equiv \delta\alpha/2b$. The propagation of the wavefront given by (15) yields a caustic surface with Cartesian coordinates (x,y,z) which are well approximated by

$$x = \frac{(\alpha + z)p\beta b}{2\alpha}\left\{(p-1)\cos\left[(p+1)\psi\right] + (p+1)\cos\left[(p-1)\psi\right]\right\}, \tag{16}$$

$$y = \frac{(\alpha + z)p\beta b}{2\alpha}\left\{(p-1)\sin\left[(p+1)\psi\right] - (p+1)\sin\left[(p-1)\psi\right]\right\}. \tag{17}$$

This is a novel result. The intersection of the plane of fixed z with the caustic surface

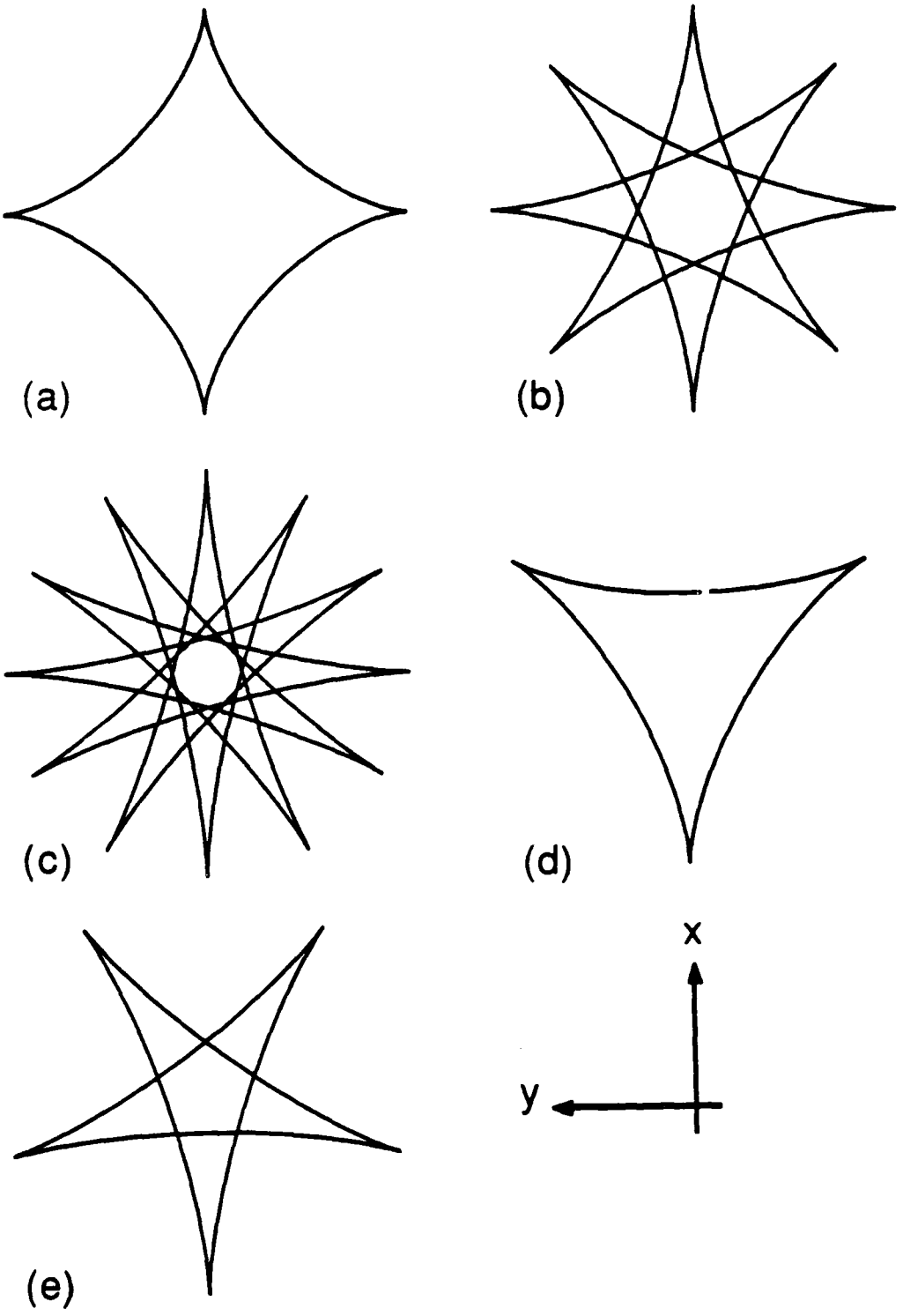

Fig. 3. Unfolded axial caustics (see text).

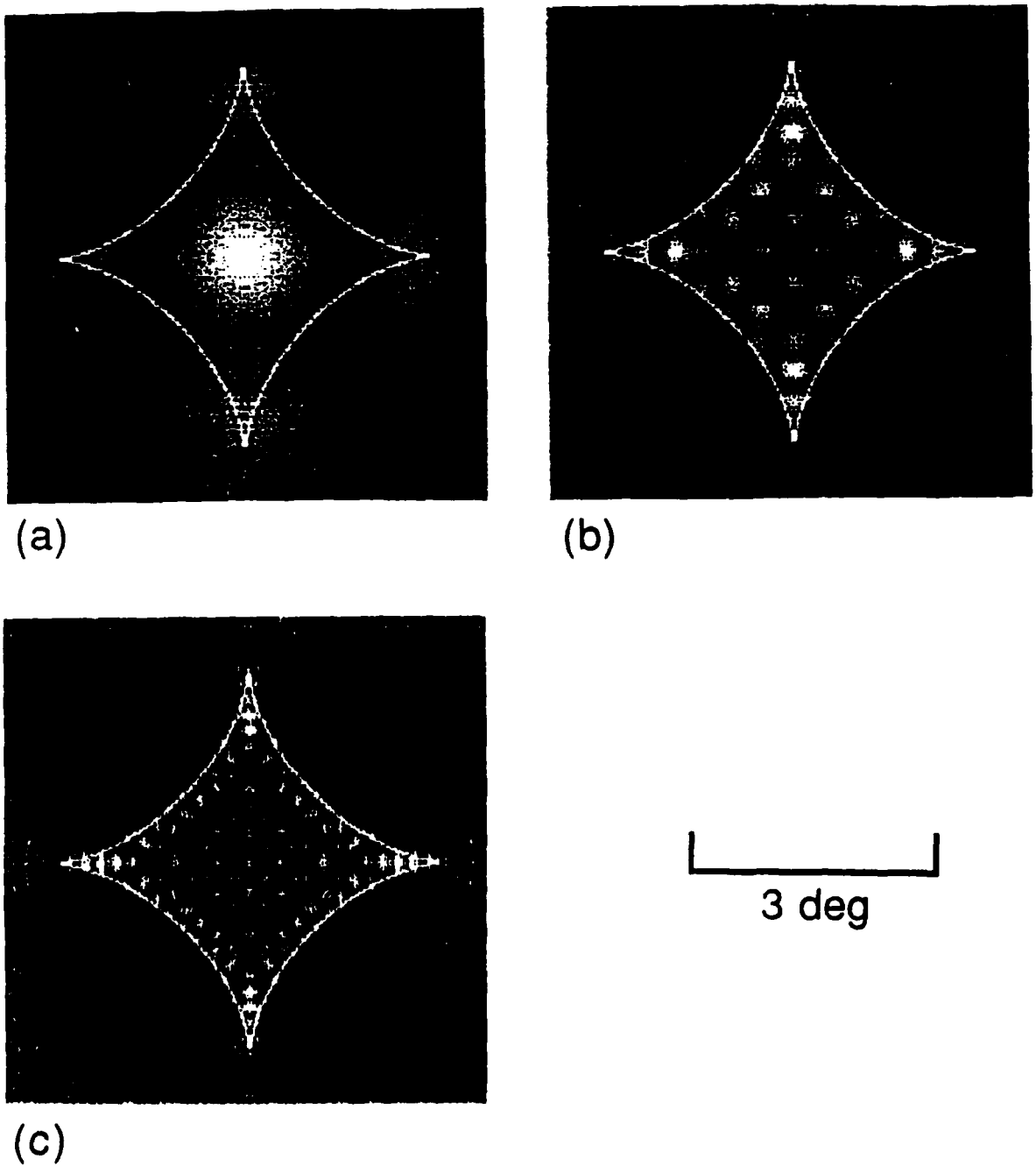

Fig. 4. Calculated wavefield patterns for astroid caustic (see text).

traces out the caustic curves shown in Fig. 3 where $p = 2, 4, 6, 3$, and 5 in (a) - (e), respectively. The specific case of $p = 2$ is the astroid curve shown in (a) and investigated previously for backscattering from freely rising bubbles in water.[4] (See also Sec. III of the present report.) The orientation of the x axis is parallel to the direction $\psi = 0$ in the polar coordinate system used to specify W. The number of (nondegenerate) cusp points for odd values of p is fewer than might have been anticipated. For example, while $p = 2$ produces 4 cusp points, Fig. 3(a), the caustic for $p = 3$, Fig. 3(d) has only 3 cusp points.

Arnott[12,13] also calculated the acoustic wavefield which decorates the caustic for the specific case of $p = 2$. To display the wavefield the squared modulus of the pressure is calculated and imaged with a grey scale where bright corresponds to large acoustic intensity. Figure 4 shows the resulting acoustic wavefield patterns for parameters $\alpha/b = 0.25$, $\delta/b = -0.02$, and (a) $kb = 100$, (b) $kb = 500$, and (c) $kb = 1000$ where $k = 2\pi/\lambda$. Superposed on these patterns is a white curve which marks the astroid caustic. For comparison, an acoustic unperturbed toroidal wavefront produces a pattern of concentric circular rings since the pressure amplitude is proportional to $J_0(kb \sin\gamma)$ where γ is the angle $\tan^{-1}[(x^2 + y^2)^{1/2}/z]$. (See, e.g., the glory scattering pattern of Lamb waves on a spherical shell.[4,5,8,9]) The wavefields are changed as a consequence of the perturbation $f(\psi)$ of the outgoing wavefront. The pattern in Fig. 4(c) near the cusp point has features like that of a Pearcey pattern discussed previously and later in Sec. II.

C. Observation of Lips Caustics in Light Backscattered from Oblate Drops

Catastrophe theory allows the caustics leaving two cusp points to join smoothly.[15] The resulting bounded caustics have the appearance of a pair of lips. (For comparison, Fig. 3(a) and (d) show the smooth joining of caustics from 4 and 3 cusp points, respectively.) With an additional flattening of the outgoing wavefront, the lips-like caustics are drawn together and the two cusp points gradually merge. The merging of cusp points is known as a "lips event" in catastrophe terminology.[15]

Nye[15] predicted that lips caustics occur in light backscattered from oblate liquid drops. Since manifestations of lips caustics are relatively unexplored and the backscattering of light or sound from penetrable spheroids is a problem of general interest, an experimental investigation of these phenomena was undertaken. The initial research was the M.S. degree project of Harry Simpson[16] though it is anticipated that the scope will be expanded to give a Ph.D. project. All experiments to date have been carried out by observing light backscattered from oblate acoustically levitated drops of water for which the refractive index $\mu = 1.332$. The first task was to build a new acoustic levitator which would allow a beam splitter to be placed close to the vibrating surfaces of the levitator. The apparatus is shown in Fig. 5. The summary of the work below is taken from a recent overview of research on optical catastrophes.[17]

Nye predicted two lips events occur in light backscattered from spheroidal drops having critical aspect ratio D/H of[5]

$$q_{L1} = \left[\mu/(2\mu-2)\right]^{1/2} \approx 1.416, \quad q_{L2} = \left[(2\mu-1)/(2\mu-2)\right]^{1/2} \approx 1.584 \qquad (18,19)$$

where D is the diameter of the drop and H is it height. (See, e.g., Fig. 3a of Ref. 18.) For $q_{L1} < q < q_{L2}$, where $q = D/H$, there are no caustics in the near backward direction. Marston's analysis of the cusp point location[18] predicts that the horizontal scattering angle θ_3 to the cusp point $\rightarrow 180°$ as $q \rightarrow q_{L1}$. That analysis indicates e.g. that if q is reduced below q_{L1} to 1.40, then $|\theta_3 - 180°| \approx 26°$.

Nye's derivations are brief so a discussion is merited. The condition for the event at q_{L1} is that paraxial rays *in the vertical plane of symmetry* are focused on the back of the drop (Fig. 6). The focal length in this plane is given by the lens maker's formula $f = \mu\rho/(\mu-1)$ where $\rho = H^2/2D$ is the vertical radius of curvature at the equator. Setting $f = D$ and solving for D/H yields Eq. (18). The condition for the event at q_{L2} is shown in Fig. 7. The internal paraxial focus F is now a distance ρ from the back side of the drop so that the reflected rays are also focused at F. Setting $\rho = D-f$ yields Eq. (19).

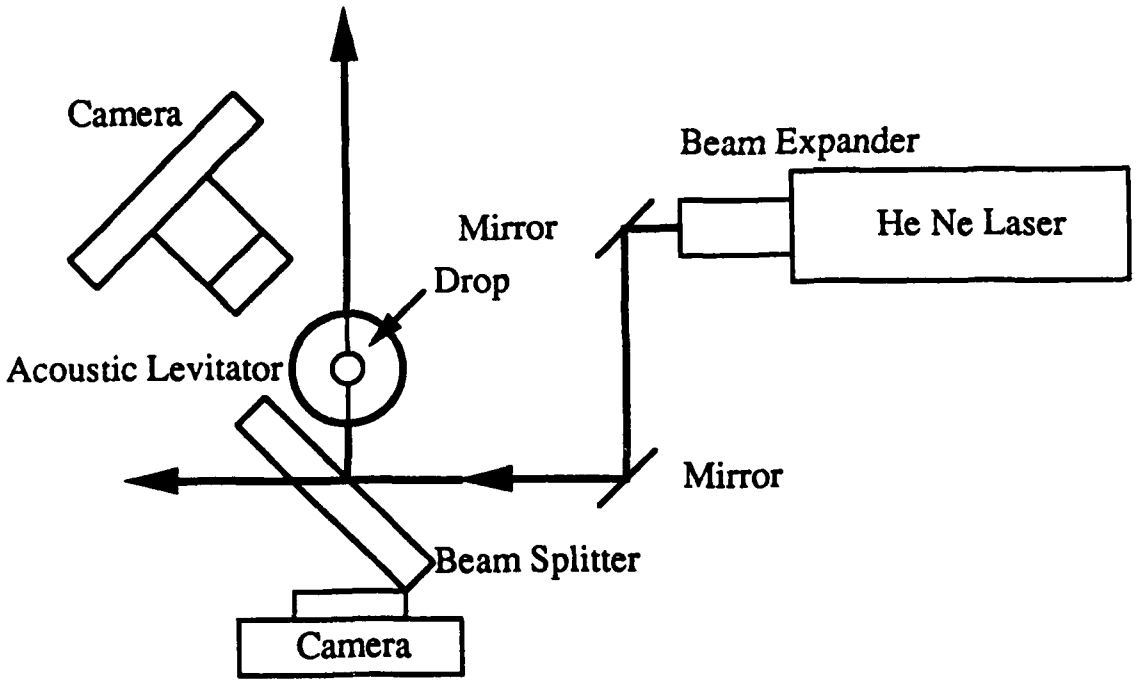

Fig. 5. Top view of apparatus. Light is backscattered from the drop through a beam splitter into a camera which records the backscattering pattern.

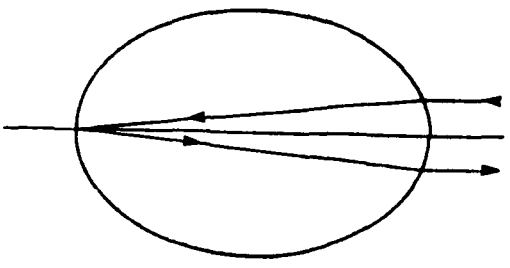

Fig. 6. Profile of oblate drop in a vertical plane containing the vertical axis of rotational symmetry. Rays are focused at the back of the drop for the 1st lips event.

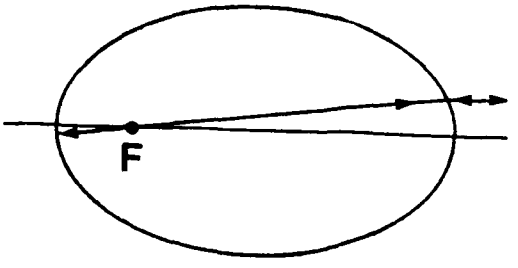

Fig. 7. Profile as in Fig. 6 but showing the focusing of rays for the 2nd lips event.

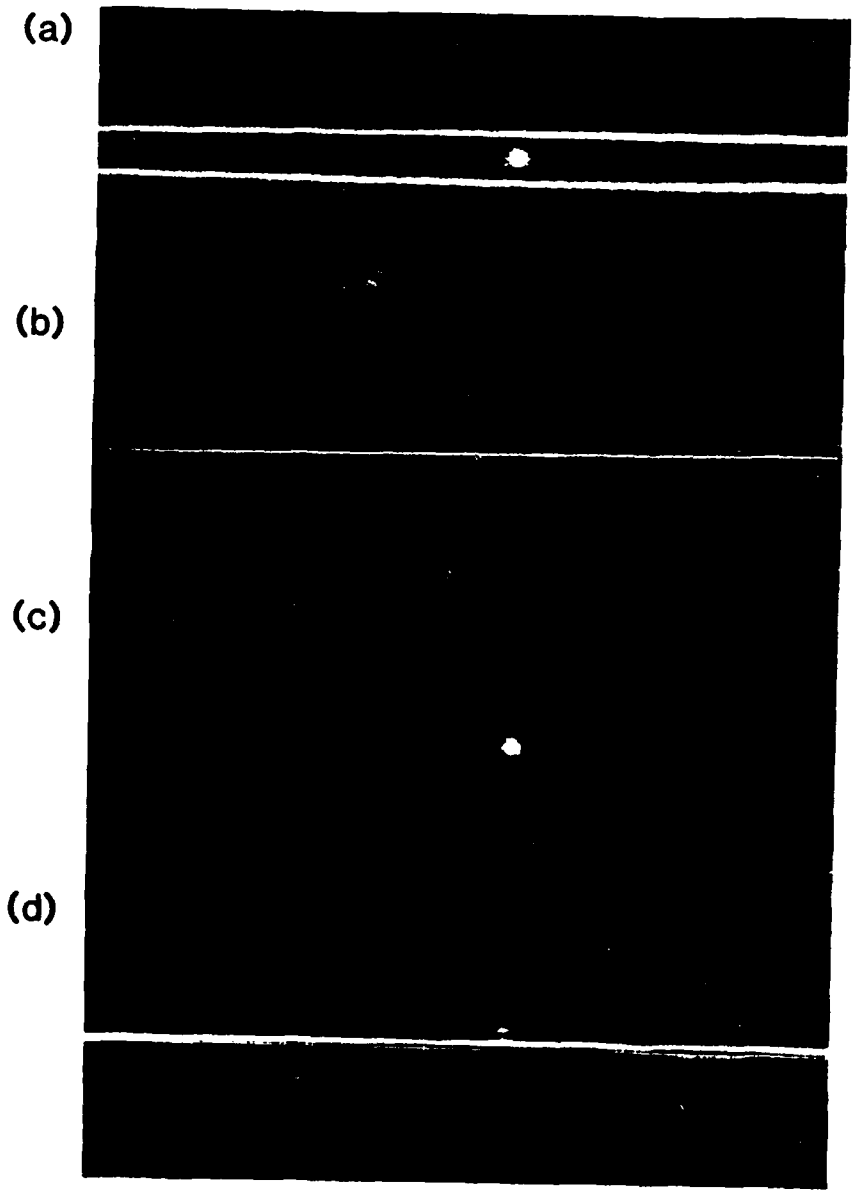

Fig. 8. Backscattering patterns for oblate drops with a diameter D and aspect ratio D/H of: (a) 1.40 mm and 1.418; (b) 1.69 mm and 1.437; (c) 1.71 mm and 1.484; and (d) 1.62 mm and 1.596. The lips caustics are distinct in (a) but not in (b). The field of view is 17°.

We have confirmed these events exist by viewing laser light backscattered from levitated drops of water.[16] The ultrasonic field for our levitator is excited by a pair of vibrating rods which face each other. This facilitates mounting a camera (focused on infinity) closer to the drop than previously possible. The incident beam reflects from a beam splitter (mounted adjacent to the rods) onto the drop. The backscattered light passes through the splitter to the camera. A second camera records the drop's profile. Figure 8 shows backscattering patterns recorded for various D/H. (The bright point visible in these is light from a distant beam dump illuminated by that part of the beam not scattered by the drop. It is useful as a fiducial mark of the backward direction.) Drops flattened by this amount from acoustic radiation pressure may have significant deviations from the perfect spheroidal shape assumed in the derivations. Hence it is appropriate to consider an optically equivalent *spheroid* (with aspect ratio q_s) where the vertical curvature at the equator ρ^{-1} matches that of the actual drop. Let q_{sj} denote the apparent q_s for the jth part of Fig. 8. *The patterns in Fig. 8 may be understood as follows*: q_{sa} is sufficiently less than q_{L1} that the lips appear as two horizontal caustic lines. These are the distinct bright lines which are displaced in (a) by vertical angle ~1.2°. The drop is flatter in (b) so that q_{sb} is much closer to q_{L1} and the horizontal caustics are nondistinct. Nevertheless, as in (a), θ_3 is not close enough to 180° for the cusp points (where the caustics terminate) to be in the field of view. (A somewhat wider field of view than the present 17° would be needed to photograph symmetric cusp points.) In (c), a slight increase of the acoustic amplitude raises q_s to $q_{sc} > q_{L1}$ so that no caustics are visible. The reason why the actual merging of symmetric cusp points at 180° would be difficult to photograph is evident by inspection of Fig. 4 of Ref. 18: the rate at which $\theta_3 \rightarrow 180°$ diverges as $q_s \rightarrow q_{L1}$. An additional flattening of the drop gives rise to a new horizontal caustic at $q_{sd} > q_{L2}$ because of the second lips event.

To facilitate a quantitative check of the theory, several drops were photographed for patterns equivalent to (a) - (d) of Fig. 8. For each photo, q_s was determined by measuring

the equatorial radius of curvature ρ and averaged with other measurements of the jth class. The resulting *averages* are $q_{sa} = 1.398 \pm 0.085$, $q_{sb} = 1.408 \pm 0.052$, $q_{sc} = 1.461 \pm 0.048$, and $q_{sd} = 1.587 \pm 0.093$. These results are consistent with the predictions that $q_{sa} < q_{L1}$, $q_{sb} \lesssim q_{L1}$, $q_{L1} \lesssim q_{sc} < q_{L2}$ and $q_{sd} \gtrsim q_{L1}$. The size of the uncertainties is indicative of the difficulty in determining ρ from photographs. The D ranged from 1.3 to 2.3 mm. In spite of the aforementioned uncertainties, the predicted sequence of lips caustics is confirmed. This is the first observation of these events for scattering from oblate objects.

D. Observations of Acoustical and Optical Transverse Cusps Produced by Reflection

In the previous Annual Report,[4] experiments are described in which a burst of ultrasound, only a few cycles in duration, was reflected from a curved polished metal surface in water. The surface was curved in the generic shape to produce transverse cusp caustic.[14,19] See. Fig. 9. Depending on the location of the receiving hydrophone, distinct echoes could be resolved in time; echoes merged when the caustic was crossed.

The research during the contract period under consideration was to explore the reflected wavefield for a quasi-steady-state incident burst of ultrasound. This work was part of the M.S. degree project of Carl Frederickson,[20] though it is anticipated that the scope will be expanded to that of a Ph.D. project. The use of long tone bursts has two advantages over the work reported in Ref. 4. (i) A theory for the steady state reflected wavefield was given by Marston[4,19] which predicts the pattern is that of a Pearcey function[14]

$$P(X,Y) = \int_{-\infty}^{\infty} \exp\left[i(s^4 + s^2X + sY)\right]ds, \qquad (20)$$

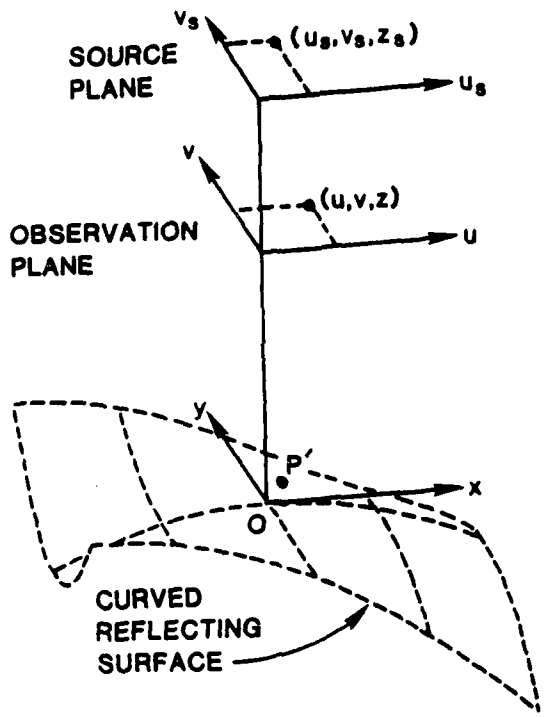

Fig. 9. The wave from a point source reflects to give a transverse cusp in the observation plane. The reflecting surface illustrated has a height relative to the xy plane of $h(x,y) = c_1x^2 + c_2y^2x$ *with* $c_1 < 0$ *and* $c_2 < 0$.

Fig. 10. (on the next page.) Observed and predicted transverse cusp caustics and wavefield patterns for a curved polished metal surface in water (all on the same scales). (a) Shows the optical caustic recorded by placing a light source in the water and scanning a photocell. (b) Shows the acoustical transverse cusp pattern for the same reflector where sound frequency is 610 kHz. (c) Shows the calculated pattern for the acoustic wavefield for that frequency of sound (see text). The horizontal width of the region displayed in (a) is roughly 9 cm while the vertical width is roughly 14 cm; $z_s \approx 133$ cm while $z \approx 48$ cm.

(a)

(b)

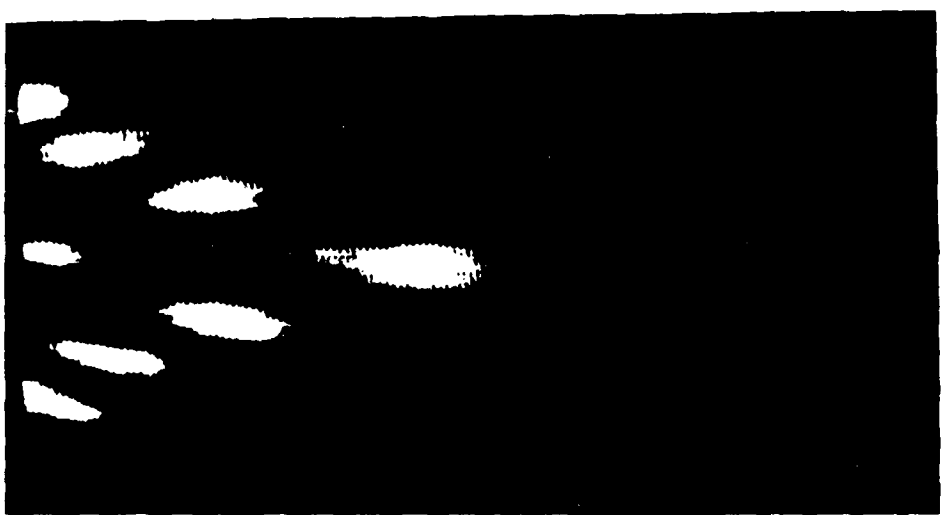

(c)

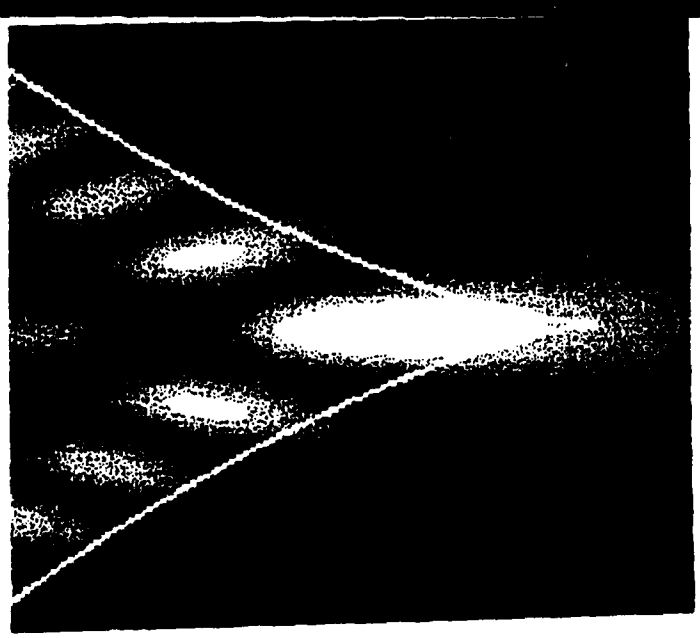

where X and Y are related to the transverse coordinates (u,v) of the observer (Fig. 9). (ii) For the laboratory scale experiments described in Ref. 4, it was difficult to fully resolve distinct echoes because of the bandwidth restrictions of the transducer and amplifier systems used. This resolution problem is avoided when studying the structure of the acoustic caustic by the present method since the incident burst is selected to be long enough (burst duration $\tau_b \gtrsim 400\ \mu s$) that all of the echoes overlap *completely* in the region of time and space sampled for the reflected wavefield. (The present method is analogous to inferring small path length differences with an interferometer instead of by direct measurement in the time domain.) Marston's theory[4,19] relates X and Y in Eq. (20) not only to (u,v,z) of the observer but also to the source coordinates (u_s, v_s, z_s), the wavelength λ, and the parameters c_j of the elevation function of the reflecting surface

$$h(x,y) = c_1x^2 + c_2y^2x + c_3y^2. \tag{21}$$

The wavefronts leaving the source at (u_s, v_s, z_s) are approximately spherical for those waves diverted toward the surface.

In the experiment, the receiver hydrophone was scanned in a raster pattern with the aid of a modified "x,y" plotter. The received signal was amplified and rectified and sampled at an appropriate time. The resulting sample-and-hold voltage produced was proportional to the pressure amplitude at the current hydrophone position. This voltage was used to modulate the intensity of an oscilloscope beam subjected to a raster scan in synchronization with the hydrophone. Figure 10(b) shows a representative photograph of the pattern on the oscilloscope which images the sound field. Bright regions correspond to the regions of greatest acoustic pressure.

The reflecting surface used was fabricated with $c_1 \approx 0$ and $c_3 \approx 0$ in Eq. (21). One approach to testing the theory would require accurate measurement of c_2, u_s, and v_s. We chose a different method which involves comparison with the optical caustic produced by placing an optical point source at the same location as the acoustic source. This was

done with the aid of an optical fiber (driven by a laser) with its output end in the water tank. The receiver hydrophone was replaced by a water-proof photo detector. The output of the detector modulates the oscilloscope. This gives the image of the optical caustic shown in Fig. 10(a). It should be emphasized that all of the geometrical properties are the same in Fig. 10(a) and (b); the difference in the patterns is primarily a consequence of λ *differing by a factor of 5200.* Let M_u and M_v denote the horizontal and vertical magnification factors for these patterns (relative to actual laboratory coordinates). For these patterns, $M_u < M_v$ while the respective values of M_u and M_v are the same in Fig. 10(a), (b), and (c). The cusp curve of the caustic is characterized by[4,19] an "opening rate." By overlaying such curves on Fig. 10(a), an empirical opening rate was determined where use is made of M_u and M_v. Then Marston's theory was used to give the surface parameter c_2 in Eq. (21) and the acoustic wavefield shown in Fig. 10(c). The agreement between Figs. 10(b) and (c) is satisfactory, though experiments are under way to repeat this comparison over a range of frequencies. For smaller acoustic λ, the structure in the pattern is more closely spaced. For one of the reflecting surfaces c_2 could be accurately estimated directly and this gave a c_2 in satisfactory agreement with the one determined optically.

To evaluate the theory, it was necessary to use a numerical algorithm to evaluate the Pearcey function, Eq. (20). Another graduate student supported by this contract, Cleon dean, participated in that accomplishment.

III. OPTICS OF BUBBLES IN WATER

A. Physical Optics of Bubbles in Water

Previous Annual Reports[4,21] have surveyed research into the physical optics of bubbles in water. Contrary to what may have been anticipated there can be significant errors if purely geometrical methods (adapted to retain phase information) are used to calculate the scattered irradiances. This is because even though bubbles are very much larger than the wavelength of light in water λ_w, the effects of diffraction are significant

near caustics and near the critical angle. Furthermore, surface coatings which can be present on bubbles in ocean water, may affect the scattering in ways which merit exploration.[4,21,22]

The emphasis on this section will be on accomplishments during the past year which are yet to be published. Marston was recently asked to give an overview of bubble optics[23] and parts of the summary below are adapted from that manuscript.

B. Brewster Angle Scattering from Bubbles: Theory and Experiment

When the electric field is polarized parallel to the plane of incidence, the Fresnel reflection coefficient of a flat clean interface vanishes when the angle of incidence is at Brewster's condition[22]

$$i_B = \arctan(n_i/n_w), \text{ Brewster scattering angle} = \theta_B = 180° - 2i_B = 106.2° \qquad (22,23)$$

where n_i and n_w are the refractive indices of air and water. Equation (23) follows from geometry and the assumption that Brewster's condition is not significantly affected by curvature provided the bubble radius $a >> \lambda_w$. This local reduction in the reflectivity manifests itself in calculated I_2, the normalized irradiance for this polarization for an uncoated bubble. This was shown in Fig. 9 of last year's Annual Report.[4] The visibility of fine structure fringes is greatly reduced when the scattering angle θ is close to 106.2°. Similar calculations done for coated bubbles predict, however, a much smaller reduction in the fringe visibility for θ near 106.2°. Consequently, if Brewster angle effects can be observed for freely rising uncoated bubbles, it is plausible that such effects could be used to optically discriminate uncoated from coated bubbles. Stefan Bäumer carried out the first observations of Brewster angle light scattering from air bubbles rising in water with the support of this contract. His M.S. thesis which describes these experiments has been issued as a Technical Report.[24]

The scattering patterns in the angular region near 106° were photographed for bubbles rising freely through distilled water. This was done to verify for the first time, that

a local reduction in fringe visibility is observable. The bubbles were illuminated by a horizontally propagating 300 mW beam from an Ar-ion laser for which the wavelength in air $\lambda_i = 514.5$ nm and $k = 2\pi n_w/(n_i\ 514\ \text{nm}) \approx 16.29\ \mu\text{m}^{-1}$. The already polarized output of the laser was made more perfectly polarized (with a horizontal E field) by passing the beam through an ellipsometer-grade polarizer. Light in the horizontal scattering plane passed through a window into a Polaroid filter and camera focused on infinity. The apparatus was generally similar to the ones used to view critical angle scattering except for changes needed to facilitate viewing the Brewster region and the reduction in the level of spurious and background scattering. After rising through the beam, the bubble floated against a glass slide and its radius was measured directly. The photographic negatives of the scattering were scanned with a microdensitometer from which an exposure E_N as a function of the scattering angle θ could be determined. The angle calibration of the photograph was achieved by use of a mirror-goniometer technique. Even with no bubble in the beam, the photograph would be weakly exposed. The smoothed irradiance pattern inferred from a background photograph will be denoted by $f(\theta)$. It was desired to compare the scattering patterns from bubbles with predictions from Mie theory for clean (uncoated) bubbles. To facilitate this comparison, it was necessary to introduce three positive adjustable parameters α,β, and C from which the normalized irradiance $I_2(\theta)$ could be inferred from the exposure $E_N(\theta)$ for a given bubble via

$$I_2(\theta) = \beta[E_N(\theta) - \alpha f(\theta) + C]. \tag{24}$$

The parameter α was selected so as to remove a component of E_N attributable to background; C was selected to eliminate an apparent offset. The scaling constant β was adjusted to facilitate comparison with a locally averaged form of $I_2(\theta)$ from Mie theory. A similar local average was performed on the "raw" $E_N(\theta)$ from the negatives so as to reduce noise associated with the graininess of each photograph.

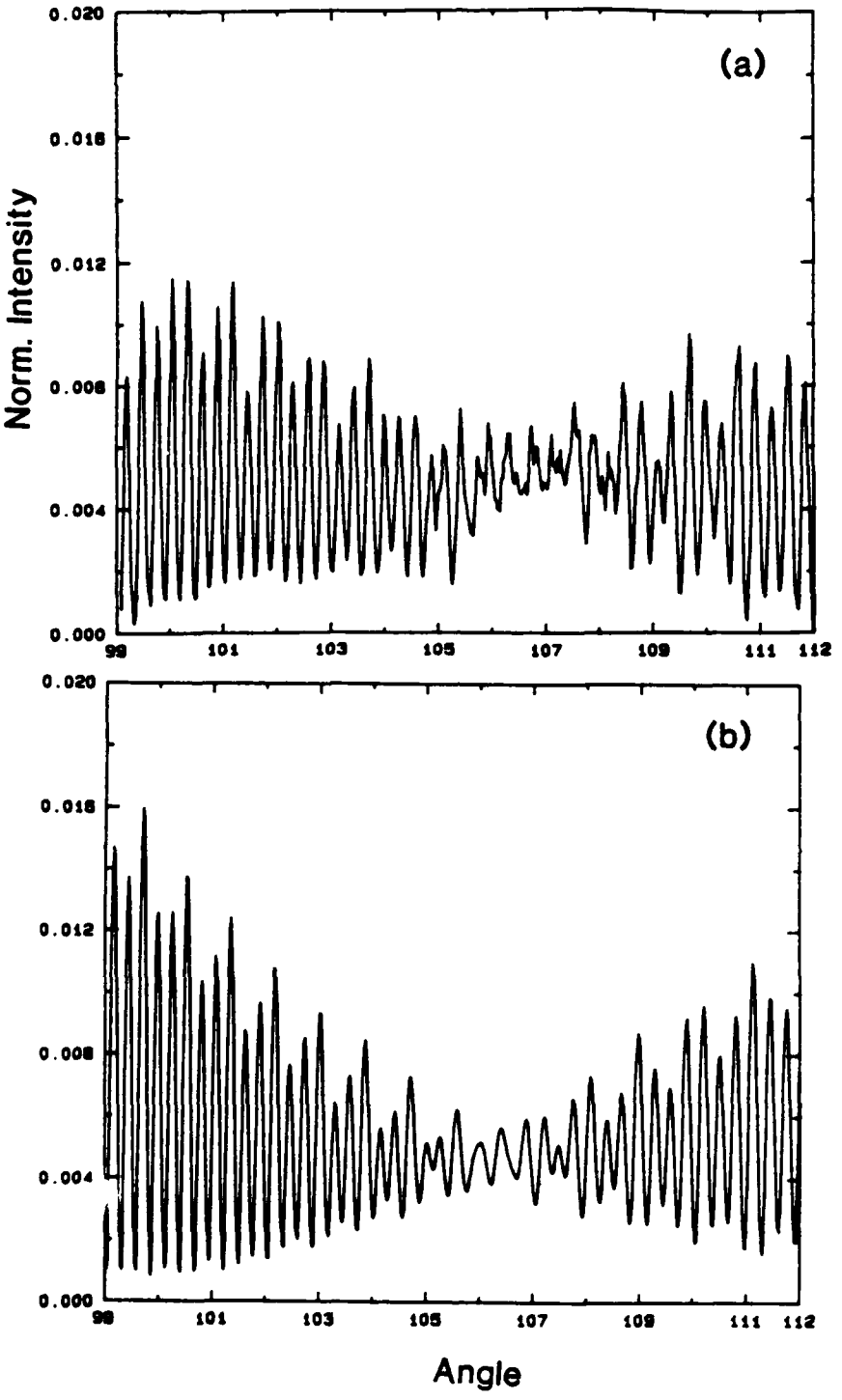

Fig. 11. Normalized irradiance for a bubble of radius 78.5 μm in green light: (a) is inferred from a photograph and confirms the local reduction of fringe visibility near the Brewster condition; (b) is a narrow angular average if I_2 from Mie theory for ka = 1278.

Figure 11 is a representative comparison of data with theory for a case where the local average was over ± 0.04°. Outside of the region from about 105° to 108°, the quasiperiod of the irradiance oscillations is fairly uniform. Measurement of that quasi-period shows that the oscillations are primarily associated with the interference of the surface reflected ray with a (far-side) 2 chord ray. For θ close to $\theta_B \approx 106°$, there is a noticeable reduction in the fringe visibility and the quasi-period changes. The reflected ray is suppressed there and the fringes can be attributed to the interference of other (weak) rays.[24] The important result is that the same general features are observable. It is noteworthy that the local reduction of the fringe visibility near θ_B is evident in the "raw" $E_N(\theta)$. Similar detailed comparisons were carried out for bubbles having radii ranging from 60 to 80 μm, while reduction in fringe visibility was noted with radii from 50 to 100 μm. Since the experiments were carried out in distilled water, no optically significant coating was expected and no evidence for such a coating was found. This confirmation of Brewster effects for uncoated bubbles suggest that the effects of a film may be observable.

Since geometric features are important near the critical scattering angle $\theta_c = 82.8°$ and θ_B, it may be argued that the ratio $\langle I_2(\theta_c)\rangle/\langle I_2(\theta_B)\rangle$ depends only weakly on ka for bubbles where $\langle\ \rangle$ denotes a local average about the indicated scattering angle. Measurement of that ratio may be useful for discrimination of bubbles from particles-in-water.[25]

C. Backscattering from Freely Rising Spherical and Spheroidal Air Bubbles in Water: Glory Scattering and the Astroid Caustic

For a spherical bubble, some of the rays incident with non-vanishing impact parameters leave the bubble scattered exactly backwards.[26] As a consequence of the azimuthal symmetry of spheres, the scattering associated with such rays is weakly focused along the backward axis. This weak focusing is generally termed "axial focusing" or "glory scattering" and manifests itself in a local enhancement of backscattering from spherical cloud droplets; the detailed cause of glory rays is different for drops and bubbles.

The shape of the backward directed wavefront is toroidal and is of the form described by $\hat{W}(s)$ in Eq. (13).

Real bubbles rising through water take on an oblate shape as a consequence of hydrodynamic forces on the bubble. For a sufficiently oblate bubble, the outgoing wavefront becomes distorted as shown in Fig. 9 of a previous Annual Report[21] and the focal properties of the scattering are changed. The wavefront shape becomes perturbed such that it is locally well approximated[12,13] by Eqs. (13) - (15) with $p = 2$ in Eq. (14). Hence the axial caustic unfolds to give an astroid caustic having the shape shown in Fig. 3(a). Because of polarization effects and the superposition of fields from several such wavefronts, the scattering patterns are much more complicated than those shown in Fig. 4 for the acoustic case.

During the contract period under consideration Arnott photographed and modeled backscattering patterns from bubbles rising through water which were sufficiently oblate to display an astroid caustic. The research is described in his Ph.D. dissertation[12] and in a short publication[27] and will be only briefly summarized here. All of his observations are of cross-polarized backscattering patterns. In the ones described in previous Annual Reports[4,21] the incident light was vertically polarized so that the polarization is *symmetric* relative to the rotational axis of the oblate bubble (since the latter axis is also vertical). In the new observations, the incident light was polarized at 45° relative to the vertical which is *asymmetric* relative to the bubble. With this change of illumination, the backscattering pattern is more intense near the cusp points of the astroid than in the previous observations. Arnott extended his previous calculation of the relevant diffraction integrals to include the case of asymmetric polarization. Figure 12 shows the observed (a) and calculated (b) pattern for asymmetric illumination of a bubble having a diameter $d \approx 654$ μm. The caustics associated with the 3 and 4 chord glory wavefronts are highlighted in (b). The theory reproduces the general features and dimensions of the observed pattern if not its detail.

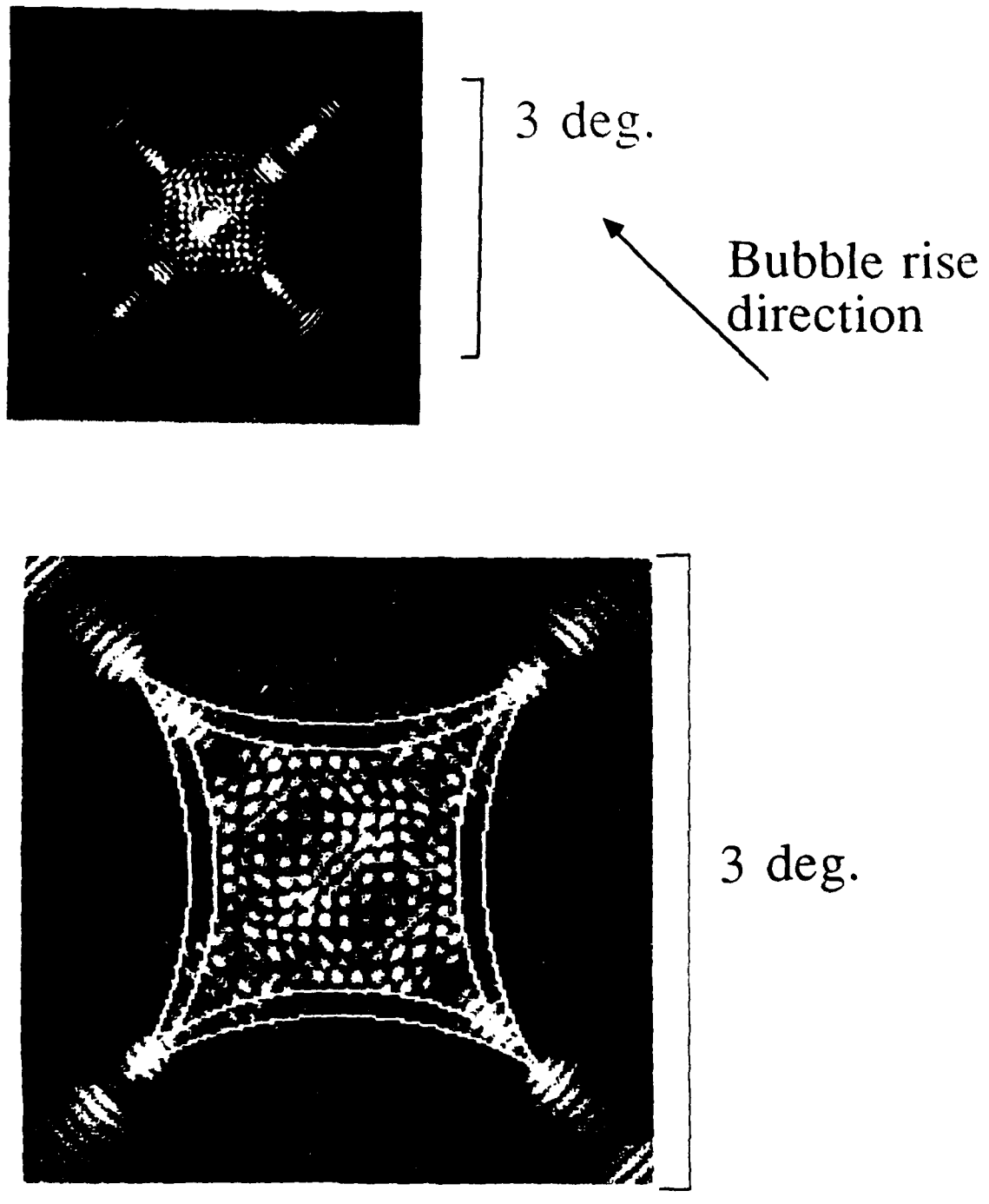

Fig. 12. Observed (a) and calculated (b) backscattering patterns for an oblate bubble rising vertically through water with a diameter $d \approx 654\ \mu m$. The vertical rise direction is shown by the arrow. The illumination was green laser light polarized at 45 deg relative to the vertical. Astroid caustics are superposed on (b).

In related work, Arnott measured the apparent caustic dimensions for patterns with vertically polarized illuminations. He used those measurements to infer the oblateness of the bubble where use is made of the optical model. The inferred oblateness is in fair agreement with the results of a hydrodynamics approximation.[12,27] This method of determining the oblateness of a rising bubble is very much more sensitive than simple photography of a rising bubble. The difference between the major and minor diameters may be inferred even when that difference is < 1%.

D. Asymptotic Series for Scattering at the Critical Angle from CAM Theory

While the physical optics approximation[28] (POA) gives a simple and quantitative understanding of coarse structure present is scattering with $\theta < \theta_c = 82.8°$, the critical value for total refection, comparisons with Mie theory[29] show that the POA noticeably underestimates the irradiance at θ_c when ka is quite large (roughly ka > 2000). The error is a consequence of the auxiliary assumptions made in the POA so that the relevant diffraction integral could be reduced to the form of a Fresnel integral.[28] To facilitate a more rigorous analysis Ferrari and Nussenzveig[30,31] extended the modified Watson transformation of the Mie series to the case of bubbles. The results is known as the *complex angular momentum* (CAM) theory. They obtained excellent agreement with angular scattering patterns computed from Mie theory.[30] The important result is an approximation for the amplitude of reflected light in terms of integrals denoted as P_F and F_F and given the names Pearcey-Fock and Fresnel-Fock integrals. The integrals depend on ka, θ, and θ_c. The integrals were evaluated numerically by Ferrari.[30]

To obtain a simple series approximation to the scattering at $\theta = \theta_c$, Cleon Dean found series expansions of P_F and F_F in the special case $\theta = \theta_c$. This work was only partially supported by this contract.[32] The contribution of the reflected light to the normalized irradiance becomes

$$I_j(\theta_c,\beta) \approx \left|\sum_{q=0}^{M_A} A_{j,q}\,\beta^{-q/6} + \sum_{q=0}^{M_B} B_{j,q}\beta^{-q/4}\right|^2, \qquad (25)$$

where $\beta = ka$, $A_{j,0} = B_{j,0} = 1/2$ and the coefficients $A_{j,q}$ and $B_{j,q}$ are complex for $q \geq 1$ and j is a polarization index. Note that $\beta^{-q/6} = 1$ and $\beta^{-q/4} = 1$ for $q = 0$. Because the analysis leading to the $A_{j,q}$ and $B_{j,q}$ is tedious, it was necessary to terminate the series at small M_A and M_B. While the form of the series is certain, some aspects of the analysis for the $A_{j,q}$ and $B_{j,q}$ with $q > 0$ are being reexamined as of the time of this writing. Some of the noteworthy features evident from inspection of Eq. (25) are (i) $I_j(\theta_c, \beta \rightarrow \infty) \rightarrow 1$ which is the correct geometric optics limit for total reflection and (ii) the leading correction to the geometric optics limit is $O(\beta^{-1/6})$. This is of fundamental interest since away from special angles, the corrections to geometrical optics are usually $O(\beta^{-1})$. Hence β must be usually large for $\theta = \theta_c$ for I_j to be close to 1. For example, for $j = 1$, which is E field parallel to the scattering plane, diffraction is especially important and $\langle I_2 \rangle$ from Mie theory has only reached 0.62 for $ka = 20000$, corresponding to a bubble radius a of 1.5 mm in red light.

This analysis constitutes a part of Cleon Dean's dissertation project which should be completed in the next few months. In addition to being a fundamental problem in scattering physics because $O(\beta^{-1/6})$ terms vanish slowly, the analysis has applications.[23] It is important for a full understanding of the unique monotone increasing relationship between scattered power and bubble radius for θ near θ_c. That relation has applications in instruments to measure bubble size and pulsation amplitudes. Furthermore, there is a close analogy with critical angle reflection of sound from curved fluid interfaces,[33] so the analysis could be extended to give an improved understanding of acoustic reflections if such is merited.

With the support of this contract C. Dean has also been working on applying wavefront tracing to a situation in catastrophe optics like that described in Ref. 18. There is no significant new progress on that problem.

IV. ACOUSTICAL PHASE CONJUGATION AND ASPECTS OF ACOUSTIC WAVEFRONT REVERSAL

A. Theory for Wavefront Reversal Via Three-Wave Mixing in a Layer of Enhanced Nonlinearity

Three-wave mixing is usually not the method of choice in *optical* phase conjugation as a consequence of dispersion.[34]. It is, however, potentially useful as a method of *acoustical* phase conjugation where a layer of bubbles is used to enhance the region of nonlinearity.[35,36] To improve our understanding of focal point locations and the relevant experimental parameters, an analysis of the difference frequency signal produced is carried out. This is summarized below. *A brief overview appears at the end of this section.*

The geometry considered is shown in Fig. 13. Let S_1 denote the location of the pump wave of radian frequency ω_1, and let S_2 denote the location of the probe wave of radian frequency ω_2. It is desired to produce a wave which converges back generally towards S_2 by way of three-wave mixing. The frequency of the reversed wave is $\omega_3 = \omega_1 - \omega_2$. The Cartesian coordinates of the jth source will be denoted by (x_j, y_j, z_j), $j = 1$ and 2 and we may take S_2 at $(0, 0, z_2)$ and S_1 at $(x_1, 0, z_1)$. The pressure due to these sources is:

$$p(x,y,z,t) = \frac{1}{2}\left[P_1 e^{i\omega_1 t} + P_2 e^{i\omega_2 t} + \text{c.c.}\right], \tag{26}$$

where c.c. denotes the complex conjugate and $P_j = A_j \exp(-ik_jR_j)$ where $k_j = \omega_j/c$, A_j is the source strength, and R_j is the distance of (x,y,z) from the S_1 or S_2.

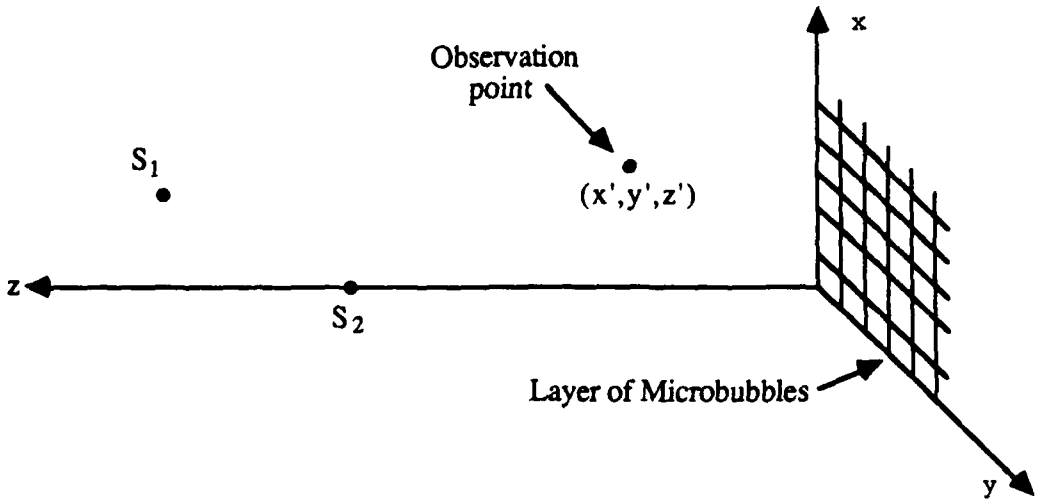

Fig. 13. Coordinate system for discussion of three-wave mixing.

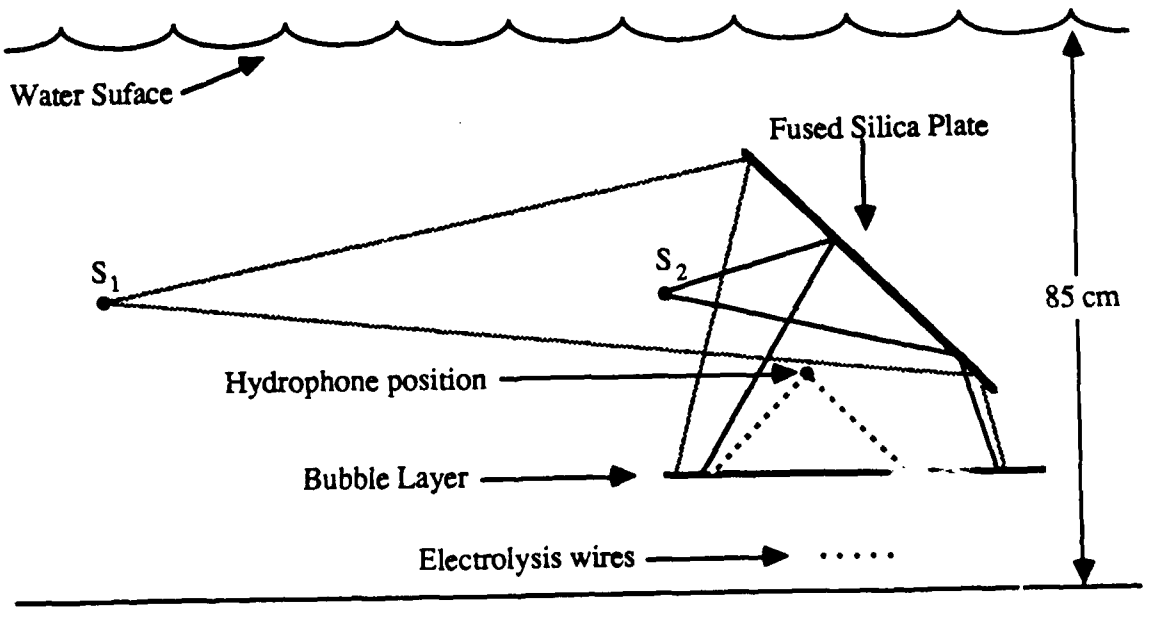

Fig. 14. Current experimental configuration.

The present calculation considers parametric sources of sound where the source strength density q is associated with a quadratic nonlinearity. Westervelt's parametric source equation reduces to[37]

$$\nabla^2 p' - \frac{1}{c^2} p'_{tt} = - \rho_o q_t , \tag{27}$$

$$q = (\rho_o c^4)^{-1} \varepsilon \partial(p^2)/\partial t \tag{28}$$

where the subscript t denotes differentiation with respect to time and hydrodynamic corrections are neglected so that Eq. (28) describes the distributed source associated with the quadratic nonlinearity in the equation of state. (In conventional notation, the nonlinearity parameter ε becomes B/2A for a homogeneous fluid.)

Inspection of Eqs. (26)-(28) shows that a component of parametrically generated wave p' oscillates at ω_3 with q being proportional to $P_2^*(x,y,z)\, P_1(x,y,z)$. The relevant component of p'(x',y',z',t) is given by the real part of

$$P_3(x',y',z') e^{i\omega_3 t} = - \int \frac{\delta(\mathbf{r}, t - |\mathbf{r}' - \mathbf{r}|/c)}{4\pi|\mathbf{r}' - \mathbf{r}|} d^3 r, \tag{29}$$

$$\delta(\mathbf{r},t) = (\omega_3)^2 P_2^* P_1 e^{i\omega_3 t} \varepsilon(\omega_1,\omega_2,\mathbf{r})/\rho_o c^4. \tag{30}$$

The integral in (29) extends over the region of the parametric source. For a bubbly liquid, ε becomes complex to take into account the phase of the response of the bubbles.[37,38] Furthermore $|\varepsilon|$ may be >> B/2A of the surrounding water and for the purposes of estimating the amplitude of the reversed wave produced in a bubble layer we may take $\varepsilon = 0$ outside of the layer. We will be interested in P_3 generated by the response of bubbles in a flat thin layer of thickness L. Let the layer lie in the plane $z = z_o$. For sufficiently thin L,

$$\varepsilon(\omega_1, \omega_2, \mathbf{r}) \approx \varepsilon(\omega_1, \omega_2)\, L\, \delta(z - z_o), \tag{31}$$

where $\delta(z - z_o)$ is a Dirac δ function so that (29) reduces to a two-dimensional integral. That P_3 describes a reversed wave may be seen by use of the parabolic (or Fresnel) approximation to simplify the various propagation distances which arise (such as the distances R_j from the jth source to a given region of the bubble layer. For simplicity we take the plane of the layer to be at $z_o = 0$ and Eqs. (29) - (31) reduce to

$$P_3(x',y',z') = \frac{-\omega_3^2 L\varepsilon(\omega_1\omega_2)A_1}{4\pi z' \rho_o c^4 z_1} J(x',y',z') \tag{32}$$

$$J \approx \frac{A_2^*}{z_2} \iint_{-\infty}^{\infty} e^{-i(x^2+y^2)F/2} e^{ixG} e^{iyH} dxdy, \tag{33}$$

$$F = \frac{k_3}{z'} + \frac{k_1}{z_1} - \frac{k_1}{z_2}, \quad G = \frac{k_1 x_1}{z_1} + \frac{k_3 x'}{z'} - \frac{k_2 x_2}{z_2}, \quad H = k_3 y'/z', \tag{34}$$

where $x_2 = 0$ for the case considered. Inspection of (33) shows that J diverges if $F = 0$, $G = 0$, and $H = 0$. These conditions may be used to directly specify the (x',y',z') where the reversed wave comes to a focus according to geometrical optics. The focus is at $y' = 0$ with

$$z' = \frac{(\omega_1 - \omega_2)}{(\omega_2/z_2) - (\omega_1/z_1)}, \quad x' = -x_1 \frac{\omega_1 z_3}{\omega_3 z_1}. \tag{35}$$

Notice that when $z_1 \to \infty$ and $x_1 = 0$ (so that the pump wave is a plane wave at normal incidence) and $\omega_1 = 2\omega_2$ (so that $\omega_3 = \omega_2$) then $z' = z_2$ and $x' = 0$. The reversed wave is focused back on S_2 which is a requirement of true phase conjugation. Specific cases of Eq. (35) for the "focal point shifts" had been derived previously by Marston[4] by less transparent methods. Equation (35) also agrees with results in Ref. 36.

A mathematical demonstration of the conjugate nature of the reversed wave in the aforementioned special case of $\omega_2 = \omega_1/2 = kc$, $z_1 \to \infty$ with $x_1 = 0$, follows by the stationary phase approximation (SPA) of J in Eq. (32) which gives

$$P_3 \approx \frac{A_2^*}{R} e^{ikR\ \mathrm{sgn}(z)}\, e^{-i(\pi/2)\mathrm{sgn}(kz)} \mathcal{G}, \tag{36}$$

$$\mathcal{G} \approx \frac{1}{2} \frac{P_1(z=0)}{\rho_o c^2} \varepsilon(\omega_1, \omega_2)\, kL, \tag{37}$$

where R is the distance of the observation point (x',y',z') from (x_2, y_2, z_2) which is the location of the "probe" source, and $z = z_2 - z'$. Since the pressure of the reversed wave is $p_3 = \mathrm{Re}[P_3 \exp(i\omega t)]$, inspection of (37) shows that the versed wave *converges* toward S_2 and, if it is allowed to pass through unobstructed, diverges when it passes beyond S_2. Inspection of (36) shows that the wave is manifestly a conjugate wave where $\mathcal{G}$ is the complex "gain" of the "phase conjugate mirror" (PCM). As $R \to 0$, the SPA breaks down and it is necessary to include the effects of diffraction. Let d denote the smaller of the diameters of the bubble layer, the pump beam, or the probe beam. By analogy with the focal properties of a converging lens of diameter d, it may be argued that the maximum pressure at the focus is roughly

$$(P_3)_{max} \approx (d^2/\lambda z_2)\, |\mathcal{G} P_2(z = 0)|, \tag{38}$$

where for the parabolic approximations used in the derivations of Eq. (32) and (33) to be applicable, the distance to the focus must be such that $d \lesssim z_2$. It is remarkable that Eqs. (37) and (38) give the same expression for the maximum pressure (apart from purely numerical factors close to unity) as the appropriate special case of Eq. (14) of Kustov et al.[36]

Some practical consequences of this analysis are: (i) Since $\rho_o c^2 \approx 22{,}000$ atm for water, generally $|\mathcal{G}| << 1$ unless $|\varepsilon|$ is quite large. Large values of $|\varepsilon|$ require a dense layer of bubbles of resonant size. For a dense layer, however, it becomes necessary to include the attenuation of the pump, probe, and reversed wave signals which was not included here. (ii) The above analysis has been extended to allow the layer to be at a plane z_o shifted from the plane $z = 0$. This introduces a phase factor $\exp(i\, 2\omega_3 z_o/c)$ in P_3 and

shows that while adjacent layers of bubbles have the same focal point, they do not necessarily have the same phase. Hence if the bubbles in a layer of finite thickness L are to produce reversed waves which add in phase, the layer should be sufficiently thin that

$$\omega_3 L/c << \pi \quad \text{which gives} \quad L << \lambda/2. \tag{39}$$

For a thin corrugated layer, L becomes the maximum amplitude of the corrugations.

This calculation is significant for the following reason. While being consistent with results in Ref. 36, the analytical methods are simpler and more closely parallel than those used in holography. Equations (37)-(38) clarify physically relevant magnitudes, though we make use of previous estimates of $|\varepsilon(\omega_1, \omega_2)|$ for bubbly water which give[38]

$$|\varepsilon(\omega_1,\omega_2)| \approx nD\lambda^4, \quad D \approx 10^{-2} \text{ to } 10^{-1}, \tag{40}$$

and n is the number of bubbles per volume per radius size increment for near resonance sizes. Inspection of Eqs. (37) and (40) shows that the following dimensionless quantity will need to be large: $|\varepsilon|kL \approx nD\lambda^3 L/2\pi$. *The analysis leading to these approximations was needed if experiments, described below, are to be viable.*

B. Experiments on Three-Wave Mixing in a Bubble Layer

A graduate student, Steve Kargl, has continued to study the generation of difference frequency signals using a modified version of the apparatus shown in Fig. 20 of the previous *Annual Summary Report*.[4] In the experiments previously described, the nonlinear layer consisted of partially-stabilized microbubbles trapped in pores (having diameters of a few μm) in a sheet of Nuclepore filter. Scans of a receiving hydrophone revealed localized enhancements of a difference frequency signal which were suggestive of the focusing of a reversed wave. The frequencies $f_j = \omega_j/2\pi$ were in the MHz range. Subsequent experiments have indicated, however, that the peaks observed were probably not due to a reversed wave. Instead, it appears that the linear scattering of the pump and probe waves from the Nuclepore sheet (and its mount) varies with hydrophone position. If

waves at frequencies ω_1 and ω_2 of sufficient intensity are incident on the hydrophone, a voltage can be produced at the difference frequency $\omega_3 = \omega_1 - \omega_2$ as a consequence of the modulation of the radiation pressure on the hydrophone; this can mask the signal of interest. The use of a Nuclepore filter as a means of stabilizing microbubbles has another drawback which we were not aware previously: in spite of the hydrophobic coating on the Nuclepore filter, the gas in the pores can dissolve over a time scale of a few hours (or less).[39]

Because of the aforementioned difficulties, other methods have been (and are being) tried for creating a layer of bubbles. The bubbles were produced by electrolysis and lower frequencies are used: typically $f_1 \approx 400$ kHz and $f_3 = f_1 - f_2$ in the range of 50 to 105 kHz. In the first of these experiments (spring, 1988) the electrolysis wires ran horizontally, one above another, in an array. The bubbles came off in roughly vertical sheets. The sheets, however, were neither thin nor flat, so that the condition given as Eq. (39) is typically violated. The signal amplitude at the difference frequency varied greatly from burst to burst, evidently as a consequence of changes in shape and composition of the bubble layer. Hence, while interference with background reflections were eliminated with this configuration, the time variability of the signal ruled out the use of simple signal averaging and the observations were inconclusive as to the focal properties of the reversed wave. Instead of using sophisticated signal processing methods to look for evidence of focusing in the signal at f_3, an alternative arrangement is being attempted which should facilitate achieving a thin stationary layer of bubbles as well as a low background.

Figure 14 is a diagram of the approach currently being tested. Bubbles are generated by electrolysis at a horizontal array of wires. They float upward and are trapped against a 46 cm x 46 cm horizontal sheet of clear Mylar having a thickness of 12 μm. The depth of the 500 gallon tank used does not permit the sheet to be in the far-field of the pump source at S_1 if S_1 is directly above the sheet. Hence the beam path was folded by using a large sheet of fused silica as an acoustic mirror. Taking $f_1 = 400$ kHz and $f_3 = 50$

kHz gives focal distances from Eq. (35) sufficiently small that the reversed wave comes to a focus before the mirror. The pump and probe amplitudes at the bubble layer have magnitudes of 10^3 Pa and 10^2 Pa, respectively and Eq. (38) suggests that the $|P_3|$ may be as large as 1 Pa, though only the general magnitude of the bubble density has been estimated. Though difference frequency signals of that magnitude have been observed, it is not yet known if they are focused. An effort is underway to automate or otherwise improve the speed at which the data is acquired. This is necessary since there are changes in the bubble layer on a time scale of a few hours as bubbles dissolve or coalesce. As expected the signal at f_3 goes away after several hours, evidently because of changes in properties of the bubble layer.

During the contract period under review, Kargl demonstrated a simple method of locating the source or focus of a diverging or converging wave. The method may give a definitive way of demonstrating the focal properties of a reversed wave, though at the time of this writing, it has only been demonstrated for sound received directly from transducers. The basic idea is that the signal is recorded for various hydrophone positions along a straight line. Next the phase is determined via a FFT of each record. From the phase as a function of position, the effective source location is determined.

During the contract period under review the experimental facility has been improved with the acquisition of a power amplifier for driving the probe wave source and a digital delay unit for timing the pump and probe wave bursts. In addition, Kargl has calibrated the principal hydrophone used.

C. Possibility of Phase Conjugation via Reflection from a Curved Vibrating Surface

In a previous *Annual Summary Report*[21] the possibility of phase conjugation via reflection from a plane vibrating surface was discussed. If sound of frequency f_2 is incident on a surface which vibrates at frequency f_1, a component of the reflected sound is

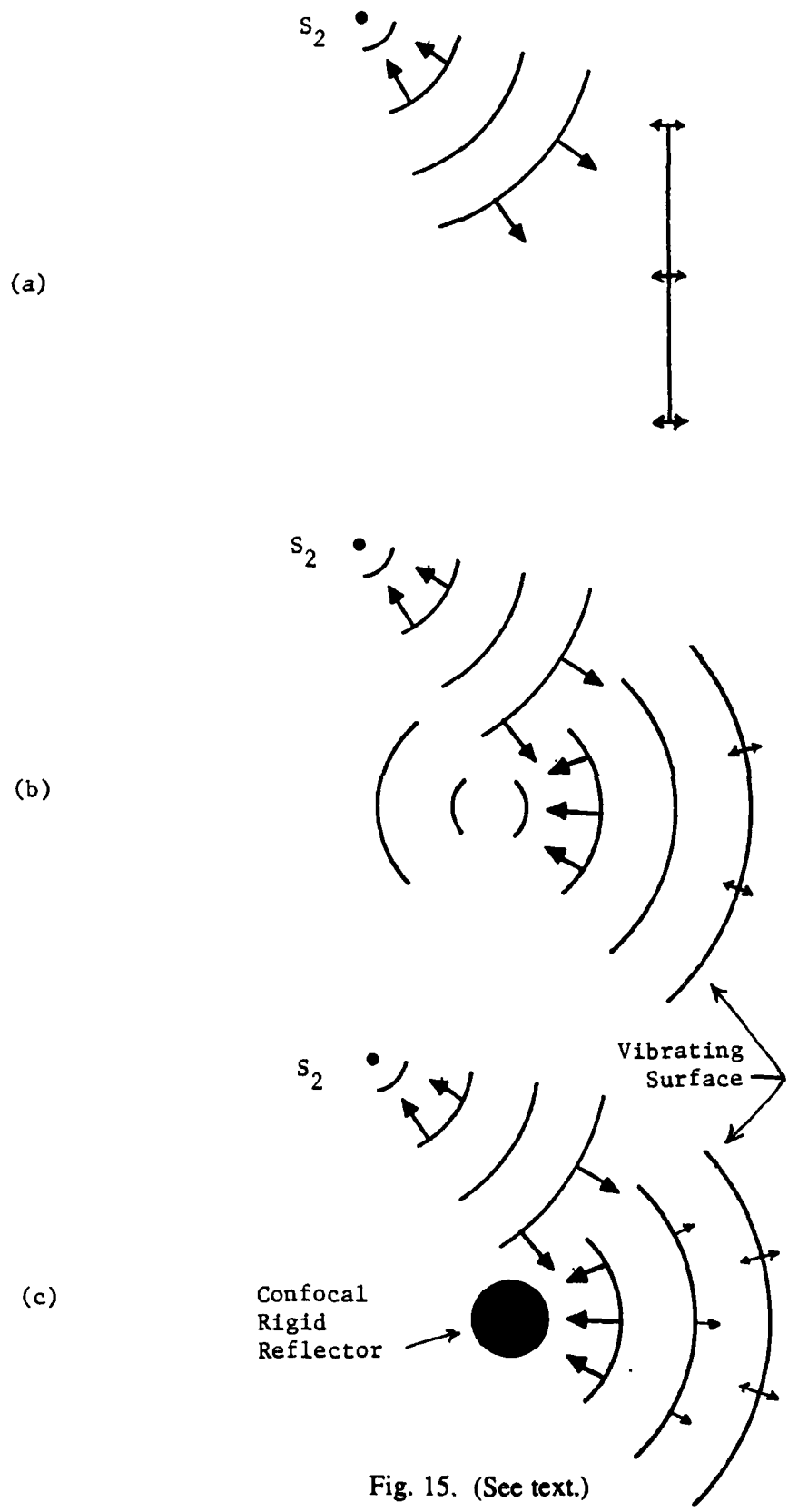

Fig. 15. (See text.)

at frequency $f_3 = f_2 - f_1$. When $f_1 = 2f_2$, that component is a conjugate wave which converges back towards the source, Fig. 15(a). The analysis leading to that result uses a paraxial approximation of phase shifts and hence the angle of incidence relative to the surface normal is not large. This mechanism was independently considered in the Soviet literature.[40]

During the contract period under review, Marston reexamined this parametric mechanism with the result that the vibrating surface need not be flat. For example, it may be a section of a sphere or a cylinder as shown in Fig. 15(b). The essential idea is that each subsection of the vibrator could be treated as the plane reflector in Fig. 15(a). The use of a curved reflector has at least two distinct advantages: (i) The strong signal radiated at frequency $f_1 = 2f_2$ may be focused away from the spatial region of interest, and hence reduce the background sound level there. (ii) The curved reflector may be made part of a resonator in which standing waves are established, Fig. 15(c). Hence the energy loss may be less than that for a plane open vibrator as in Fig. 15(a).

Independently, an analysis of a related problem recently appeared in the Soviet literature.[41] Sound of frequency f_2 is incident (from the outside) on a sphere vibrating at a frequency $f_1 = 2f_2$. A component of the scattered wave is predicted to be a conjugate wave at frequency f_2 directed towards the source.

V. REFERENCES

1. V. A. Borovikov and N. D. Veksler, "Scattering of sound waves by smooth convex elastic cylindrical shells," Wave Motion **7**, 143-152 (1985).
2. K. L. Williams and P. L. Marston, "Backscattering from an elastic sphere: Sommerfeld-Watson transformation and experimental confirmation," J. Acoust. Soc. Am. **78**, 1093-1102 (1985); **79**, 2091(E) (1986).
3. K. L. Williams and P. L. Marston, "Synthesis of backscattering from an elastic sphere using the Sommerfeld-Watson transformation and giving a Fabry-Perot analysis of resonances," J. Acoust. Soc. Am. **79**, 1702-1708 (1986).
4. P. L. Marston, "Research on Acoustical Scattering, Diffraction Catastrophes, Optics of Bubbles, Photoacoustics, and Acoustical Phase Conjugation," Annual Summary Report, issued Sept. 1987 (Defense Technical Information Center, AD-A185785) 84 pages.

5. P. L. Marston, "GTD for backscattering from elastic spheres and cylinders in water, and the coupling of surface elastic waves with the acoustic field," J. Acoust. Soc. Am. **83**, 25-37 (1988).

6. P. L. Marston and K. L. Williams, "GTD for backscattering from elastic objects in water: Phase of the coupling coefficient and a simplified synthesis of the form function," J. Acoust. Soc. Am. Suppl. **83**, 94 (1988).

7. P. L. Marston, "Coupling of sound with surface waves on fluid-loaded elastic objects described by a generalization of GTD," J. Acoust. Soc. Am. Suppl. **82**, 89 (1987).

8. S. G. Kargl and P. L. Marston, "Observations and modeling of the backscattering of short tone bursts from a spherical shell: Lamb wave echoes, glory,and axial reverberations," J. Acoust. Soc. Am. (accepted for publication).

9. P. L. Marston and S. G. Kargl, "Backscattering of sound from an empty spherical shell in water," in *Shock Wave Compression of Condensed Matter* [Proceedings of a Symposium in Honor of George E. Duvall, Pullman, WA, Sept. 1988] edited by Y. M. Gupta (Shock Dynamics Lab., Washington State University, Pullman, 1988) pp. 58-64.

10. *For example*: L. Flax, G. C. Gaunaurd, and H. Überall, "Theory of Resonance Scattering," in Physical Acoustics edited by W. P. Mason and R. N. Thurston (Academic, New York, 1981), Vol. 15, pp. 191-294, Eq. (18).

11. H. M. Nussenzveig, *Causality and Dispersion Relations* (Academic, N.Y., 1972) pp. 54-72; N. G. van Kampen, Phys. Rev. **89**, 1072-1079 (1953).

12. W. P. Arnott, "Generalized Glory Scattering from Spherical and Spheroidal Bubbles in Water: Unfolding Axial Caustics with Harmonic Angular Perturbations of Toroidal Wavefronts," Ph.D. dissertation, Washington State University (Aug. 1988); this will be issued as a Technical Report.

13. W. P. Arnott and P. L. Marston, "Unfolding axial caustics of glory scattering with harmonic angular perturbations of toroidal wavefronts," J. Acoust. Soc. Am. (submitted August 1988).

14. P. L. Marston, "Transverse cusp diffraction catastrophes: Some pertinent wavefronts and a Pearcey approximation to the wavefield," J. Acoust. Soc. Am. **81**, 226-232 (1987).

15. J. F. Nye, "Rainbow scattering from spheroidal drops—an explanation of the hyperbolic umbilic foci," Nature (London) **312**, 531-532 (1984).

16. H. J. Simpson, "The Lips Event for Light Backscattered from Levitated Water Drops," M.S. degree project report, Washington State University Physics Department (July 1988).

17. P. L. Marston, C. E. Dean, and H. J. Simpson, "Light Scattering from Spheroidal Drops: Exploring Optical Catastrophes and Generalized Rainbows," *Proceedings of the Third International Colloquium on Drops and Bubbles* (submitted, September 1988).

18. P. L. Marston, "Cusp diffraction catastrophe from spheroids: generalized rainbows and inverse scattering," Opt. Lett. **10**, 588-590 (1985).

19. P. L. Marston, "Surface shapes giving transverse cusp catastrophes in acoustic or seismic echoes," in *Acoustical Imaging Vol. 16*, edited by L. W. Kessler (Plenum, New York, 1988) pp. 579-588.

20. C. K. Frederickson, "Observation of Acoustical and Optical Transverse Cusp Catastrophes Produced by Reflection from a Curved Metal Surface in Water," M.S. degree project report, Washington State University Physics Department (July 1988).

21. P. L. Marston, "Research on Acoustical Scattering, Diffraction Catastrophes, Optics of Bubbles, Photoacoustics, and Acoustical Phase Conjugation," Annual Summary Report, September 1986 (Defense Technical Information center, AD-A174401) 48 pages.

22. P. L. Marston, S. C. Billette, and C. E. Dean, "Scattering of light by a coated bubble in water near the critical and Brewster scattering angles," in *Ocean Optics IX*, M. A. Blizard, ed., *Proc. SPIE* **925**, 296-307 (1988).

23. P. L. Marston, W. P. Arnott, S. M. Bäumer, C. E. Dean, and B. T. Unger, "Optics of Bubbles in Water: Scattering Properties, Coatings, and Laser Radiation Pressure," *Proceedings of the Third International Colloquium on Drops and Bubbles* (submitted September 1988).

24. S. M. Bäumer, "Observation of Brewster angle light scattering from air bubbles rising in water" (M.S. thesis, Washington State University, 1988) issued as a Technical Report, September 1988 (D.T.I.C. No. AD-).

25. P. L. Marston, "Light Scattering Theory for Bubbles in Water: Inverse Scattering, Coated Bubbles, and Statistics," Final Report Contract N00014-86-K-0242 issued November 1986 (Defense Technical Information Center, AD-A174997) 55 pages.

26. W. P. Arnott and P. L. Marston, "Optical glory of small freely-rising gas bubbles in water: Observed and computed cross-polarized backscattering patterns," J. Opt. Soc. Am. **A5**, 496-506.

27. W. P. Arnott and P. L. Marston, "Backscattering of laser light from freely rising spherical and spheroidal air bubbles in water," in *Ocean Optics IX*, M. A. Blizard, ed., *Proc. SPIE* **925**, 326-333 (1988).

28. P. L. Marston and D. L. Kingsbury, J. Opt. Soc. Am. **71**, 192-16, 917 (1981).

29. D. L. Kingsbury and P. L. Marston, J. Opt. Soc. Am. **71**, 358-361 (1981).

30. N. F. Ferrari, Jr., "Espalhamento de Mie na Vizinhanca do Angulo Critico," Ph.D. thesis, University of São Paulo Brazil, 1983 (in Portuguese).

31. H. M. Nuzzenzveig, "Recent developments in high-frequency scattering," Rev. Bras. Fiz. (Brazilian Reviews of Physics, special issue) 302-320 (1984).

32. From September 1987 through February 1988, the work of Cleon Dean on this project was supported entirely by a $10,000 contract (N00014-87-K-6008) with the Naval Ocean Research and Development Activity. That contract, based on the proposal entitled "Practical Computations of the Scattering of Light from Bubbles in Water (Part 2)" was in effect from September 1, 1987 through March 31, 1988. That contract also supported other calculations of a practical nature carried out by Marston.

33. P. L. Marston and D. L. Kingsbury, "Acoustic Scattering from Fluid Spheres: Diffraction and Interference Near the Critical Scattering Angle," J. Acoust. Soc. Am. **70**, 1488-1495 (1981).

34. D. M. Pepper, "Nonlinear optical phase conjugation," in Laser Handbook Vol. 4, ed. by M. L. Stitch and M. Bass (North-Holland, Amsterdam, 1985) pp. 333-485.

35. L. M. Kustov et al., "Phase conjugation of an acoustic wave at a bubble layer," Sov. Phys. Acoust. **31**, 517-518 (1985).

36. L. M. Kustov et al. "Nonlinear sound scattering by a bubble layer," Sov. Phys. Acoust. **32**, 500-503 (1986).

37. A. L. Polyakova and G. Y. Sil'vestrova, "Parametric radiator operating in a medium containing gas bubbles," Sov. Phys. Acoust. **26**, 441-443 (1980).

38. Y. A. Kobelev and A. M. Sutin, "Difference-frequency sound generation in a liquid containing bubbles of different sizes," Sov. Phys. Acoust. **26**, 485-487 (1981); Eqs. (13) and (14).

39. J. A. Rooney, Jet Propulsion Laboratory (personal communication).

40. L. M. Lyamshev, "Distinctive features of the scattering and radiation of sound by periodically moving plates and shells," Sov. Phys. Acoust. **30**, 237-238 (1984); see also papers cited in Ref. 21.

41. L. M. Lyamshev and P. V. Sakov, "Phase conjugation in nonlinear sound scattering by a pulsating sphere," Sov. Phys. Acoust. **34**, 68-72 (1988).

OFFICE OF NAVAL RESEARCH

PUBLICATIONS / PATENTS / PRESENTATIONS / HONORS REPORT

FOR

1 OCTOBER 1987 through 30 SEPTEMBER 1988

****

CONTRACT N00014 - 85-C-0141

R&T No. 4126934

TITLE OF CONTRACT: Propagation and Effects of Acoustical and Optical Waves

NAME(S) OF PRINCIPAL INVESTIGATOR(S): Philip L. Marston

NAME OF ORGANIZATION: Washington State University

ADDRESS OF ORGANIZATION: Department of Physics, Washington State University
Pullman, WA 99164-2814

****

PAPERS SUBMITTED TO REFEREED JOURNALS
(Not yet published)

1. S. G. Kargl and P. L. Marston, "Observations and modeling of the backscattering of short tone bursts from a spherical shell: Lamb wave echoes, glory, and axial reverberations," *Journal of the Acoustical Society of America* (submitted June 1988).

2. W. P. Arnott and P. L. Marston, "Unfolding axial caustics of glory scattering with harmonic angular perturbations of toroidal wavefronts," *Journal of the Acoustical Society of America* (submitted August 1988).

3. P. L. Marston, W. P. Arnott, S. M. Bäumer, C. E. Dean, and B. T. Unger, "Optics of Bubbles in Water: Scattering Properties, Coatings, and Laser Radiation Pressure," *Proceedings of the Third International Colloquium on Drops and Bubbles* (manuscript will be reviewed by a referee); research partially supported by the Naval Ocean Research and Development Activity.

4. P. L. Marston, C. E. Dean, and H. J. Simpson, "Light Scattering from Spheroidal Drops: Exploring Optical Catastrophes and Generalized Rainbows," *Proceedings of the Third International Colloquium on Drops and Bubbles* (manuscript will be reviewed by a referee).

PAPERS PUBLISHED IN REFEREED JOURNALS

1. P. L. Marston, "GTD for backscattering from elastic spheres and cylinders in water, and the coupling of surface elastic waves with the acoustic field," *Journal of the Acoustical Society of America* **83**, 25-37 (1988).

2. B. T. Unger and P. L. Marston, "Optical levitation of bubbles in water by the radiation pressure of a laser beam: an acoustically quiet levitator," *Journal of the Acoustical Society of America* **83**, 970-975 (1988).

3. W. P. Arnott and P. L. Marston, "Optical glory of small freely-rising gas bubbles in water: Observed and computed cross-polarized backscattering patterns," *Journal of the Optical Society of America* **A5**, 496-506.

PAPERS PUBLISHED IN NON-REFEREED JOURNALS

1. P. L. Marston, "Wavefront geometries giving transverse cusp and hyperbolic umbilic foci in acoustic shocks," in *Shock Waves in Condensed Matter 1987*, edited by S. C. Schmidt and N. C. Holmes (Elsevier Science Publishers, Amsterdam, 1988) pp. 203-206.

2. P. L. Marston, S. C. Billette, and C. E. Dean, "Scattering of light by a coated bubble in water near the critical and Brewster scattering angles," in *Ocean Optics IX*, M. A. Blizard, ed., *Proc. SPIE* **925**, 296-307 (1988); partially supported by the Naval Ocean Research and Development activity.

3. W. P. Arnott and P. L. Marston, "Backscattering of laser light from freely rising spherical and spheroidal air bubbles in water," in *Ocean Optics IX*, M. A. Blizard, ed., *Proc. SPIE* **925**, 326-333 (1988).

4. B. T. Unger and P. L. Marston, "Optically stimulated sound from oil drops and gas bubbles in water: thermal and radiation pressure optoacoustic mechanisms," in *Ocean Optics IX*, M. A. Blizard, ed., *Proc. SPIE* **925**, 326-333 (1988).

5. P. L. Marston and S. G. Kargl, "Backscattering of sound from an empty spherical shell in water," in *Shock Wave Compression of Condensed Matter* [Proceedings of a Symposium in Honor of George E. Duvall, Pullman, WA, Sept. 1988] edited by Y. M. Gupta (Shock Dynamics Lab., Washington State University, Pullman, 1988) pp. 58-64.

TECHNICAL REPORTS PUBLISHED

1. S. M. Bäumer, "Observation of Brewster angle light scattering from air bubbles rising in water" (M.S. thesis, Washington State University, 1988) to be issued as a Technical Report, September 1988.

Note: In the "Publications, Patents, ... Report" for 1987 the following item was listed without the DTIC Accession No. It is relisted here since that information is now known:

P. L. Marston, "Research on Acoustical Scattering, Diffraction Catastrophes, Optics of Bubbles, Photoacoustics, and Acoustical Phase Conjugation," Annual Summary Report, issued September 1987 (Defense Technical Information Center, Alexandria, VA, Accession No. AD-A185785) 84 pages.

BOOKS (AND SECTIONS THEREOF) SUBMITTED FOR PUBLICATION

N/A

BOOKS (AND SECTIONS THEREOF) PUBLISHED

N/A

PATENTS FILED

N/A

PATENTS GRANTED

N/A

INVITED PRESENTATIONS AT TOPICAL OR SCIENTIFIC/TECHNICAL SOCIETY CONFERENCES

1. *Keynote/Invited Paper*, P. L. Marston (with contributions from W. P. Arnott, S. M. Bäumer, C. E. Dean, and B. T. Unger) "Optics of Bubbles in Water: Scattering Properties, Coatings, and Laser Radiation Pressure," Third International Colloquium on Drops and Bubbles (Monterey, September 1988); Research partially supported by the Naval Ocean Research and Development Activity.

2. *Invited Paper*, P. L. Marston, C. E. Dean, and H. J. Simpson, "Light Scattering from Spheroidal Drops: Exploring Optical Catastrophes and Generalized Rainbows," Third International Colloquium on Drops and Bubbles (Monterey, September 1988).

3. *Invited address*; P. L. Marston, "Generalization of the geometrical theory of diffraction (GTD) to describe backscattering of sound from elastic objects in water," Naval Ocean Research and Development Activity, Distinguished Lecturer Series (Mississippi, January 1988).

2. *Invited address*; P. L. Marston, "GTD for Backscattering of Sound, Catastrophes, and Optics of Coated Bubbles," Naval Coastal Systems Center, Distinguished Scientist Series (Florida, April 1988); Research partially supported by the Naval Ocean Research and Development Activity.

HONORS/AWARDS/PRIZES

N/A

GRADUATE STUDENTS SUPPORTED UNDER CONTRACT FOR YEAR ENDING 30 SEPTEMBER 1988

1. William Patrick Arnott (Ph.D. Physics, August 1988)
2. Stefan M. Bäumer (M.S. Physics, August 1988)
3. Cleon E. Dean (Ph.D. Candidate, Physics)
4. Carl K. Frederickson (M.S. Physics, August 1988; Ph.D. Candidate)
5. Steven G. Kargl (Ph.D. Candidate)
6. Harry J. Simpson (M.S. Physics, August 1988; Ph.D. Candidate)

POSTDOCTORAL SUPPORTED UNDER CONTRACT FOR YEAR ENDING 30 SEPTEMBER 1988

N/A

CONTRIBUTED PRESENTATIONS AT TOPICAL OR SCIENTIFIC/TECHNICAL CONFERENCES

1. P. L. Marston, "Focal-point shifts for the reversed wave in acoustical phase conjugation experiments: Paraxial analysis and analogy with optical holography," [J. Acoust. Soc. Am. Suppl. **82**, 12 (1987)], Acoustical Society of America (Miami, November 1987).

2. P. L. Marston, "Coupling of sound with surface waves on fluid-loaded elastic objects described by a generalization of GTD," [J. Acoust. Soc. Am. Suppl. **82**, 89 (1987)], Acoustical Society of America (Miami, November 1987).

3. P. L. Marston and C. K. Frederickson, "Transverse cusp caustics produced by reflection and transmission: The caustic surface and optical simulations," [J. Acoust. Soc. Am. Suppl. **82**, 102 (1987)], Acoustical Society of America (Miami, November 1987).

4. P. L. Marston, "Weak foci in three-dimensional acoustic shocks and shock stability," [Bull. Am. Phys. Soc. **32**, 2107 (1987)], APS Division of Fluid Dynamics (Eugene, OR, November 1987).

5. W. Arnott and P. Marston, "Backscattering of laser light from freely rising spherical and spheroidal bubbles in water," [Bull. Am. Phys. Soc. **32**, 2104 (1987)], APS Division of Fluid Dynamics (Eugene, OR, November 1987).

6. P. L. Marston and B. T. Unger, "Optical levitation of bubbles in water by the radiation pressure of a laser beam," APS Division of Fluid Dynamics (Eugene, OR, November 1987).

7. P. L. Marston, S. C. Billette, and C. E. Dean, "Scattering of light by a coated bubble in water near the critical and Brewster scattering angles," presented at Ocean Optics IX (Orlando, FL, April 1988); Research partially supported by the Naval Ocean Research and Development Activity.

8. W. P. Arnott and P. L. Marston, "Backscattering of laser light from freely rising spherical and spheroidal air bubbles in water," presented at Ocean Optics IX (Orlando, FL, April 1988).

9. B. T. Unger and P. L. Marston, "Optically stimulated sound from oil drops and gas bubbles in water: thermal and radiation pressure optoacoustic mechanisms," presented at Ocean Optics IX (Orlando, FL, April 1988).

10. P. L. Marston and C. K. Frederickson, "Transverse cusp and hyperbolic umbilic caustics produced by reflection and transmission: optical experiments and caustic surfaces," presented at Wave Propagation and Scattering in Varied Media (SPIE Conference 927, Orlando, FL, April 1988).

11. P. L. Marston, "Weak foci in three-dimensional linear shock waves and the stability of real shock waves," [J. Acoust. Soc. Am. Suppl. **83**, 5 (1988)], Acoustical Society of America (Seattle, May 1988).

12. P. L. Marston and K. L. Williams, "GTD for backscattering from elastic objects in water: Phase of the coupling coefficient and a simplified synthesis of the form function," [J. Acoust.Soc. Am. Suppl. **83**, 94 (1988)], Acoustical Society of America (Seattle, May 1988); K. L. Williams supported by the Naval Coastal Systems Center.

13. W. P. Arnott and P. L. Marston, "Harmonic angular perturbation of a toroidal wavefront: A simple unfolding of an axial caustic," [J. Acoust. Soc. Am. Suppl. **83**, 59(1988)], Acoustical Society of America (Seattle, May 1988).

14. C. E. Dean, W. P. Arnott, and P. L. Marston, "Principal curvatures of general wavefronts and of reflecting or refracting surfaces," [J. Acoust. Soc. Am. Suppl. **83**, 59 (1988)], Acoustical Society of America (Seattle, May 1988).

15. S. M. Bäumer and P. L. Marston, "Brewster angle light scattering from bubbles in water: Observations and potential applications to the acoustics of natural microbubbles," [J. Acoust. Soc. Am. Suppl. **83**, 108-109 (1988)], Acoustical Society of America (Seattle, May 1988).

16. S. G. Kargl and P. L. Marston, "Acoustical phase conjugation experiments: the generation of a reversed wave through three-wave mixing in a layer of stabilized microbubbles," [J. Acoust. Soc. Am. Suppl. **83**, 5 (1988)], Acoustical Society of America (Seattle, May 1988).

17. P. L. Marston and S. G. Kargl, "Backscattering of sound from an empty spherical shell in water," in *Shock Wave Compression of Condensed Matter* [Proceedings of a Symposium in Honor of George E. Duvall, Pullman, WA, Sept. 1988] edited by Y. M. Gupta (Shock Dynamics Lab., Washington State University, Pullman, 1988) pp. 58-64.

REPORTS DISTRIBUTION FOR ONR PHYSICS DIVISION, UNCLASSIFIED CONTRACTS

Director
Defense Advanced Research Projects Agency
1400 Wilson Blvd.
Arlington, VA 22209-2309 — 1 copy

Office of Naval Research
Physics Division Office (Code 1112)
800 North Quincy Street
Arlington, VA 22217-5000 — 2 copies

Office of Naval Research
Director, Technology (Code 20)
800 North Quincy Street
Arlington, VA 22217-5000 — 1 copy

Naval Research Laboratory
Department of the Navy (Code 2625)
Washington, D.C. 20375-5000 — 1 copy

Office of the Director of Defense
Research and Engineering
The Pentagon, Rm. 3E 1006
Washington, D.C. 20301 — 1 copy

U.S. Army Research Office
Box 12211
Research Triangle Park
North Carolina 27709-2211 — 2 copies

Defense Technical Information Center
Cameron Station
Alexandria, VA 22314 — 2 copies

Director
National Bureau of Standards
Attn: Technical Library (Admin B-01)
Gaithersburg, MD 20899 — 1 copy

Commander
U.S. Army
Attn: Technical Library (STRBE-BT)
Fort Belvoir, VA 22060-5606 — 1 copy

ODDR&E Advisory Group on Electron Devices
201 Varick Street, 11th Floor
New York, NY 10014-4877 — 1 copy

Air Force Office of Scientific Research
Department of the Air Force
Bolling AFB, D.C. 22209 — 1 copy

Air Force Weapons Laboratory
Technical Library
Kirtland Air Force Base
Albuquerque, NM 87117 — 1 copy

Lawrence Livermore Laboratory
Attn: Dr. W. P. Kruplin
P.O. 808
Livermore, CA 94550 — 1 copy

Harry Diamond Laboratories
Technical Library
2800 Powder Mill Road
Adelphi, MD 20783 — 1 copy

Naval Weapons Center
Technical Library (Code 753)
China Lake, CA 93555 — 1 copy

Naval Underwater Systems Center
Technical Center
New London, CT 06320 — 1 copy

Commandant of the Marine Corps
Scientific Advisor (Code RD-1)
Washington, D.C. 20380 — 1 copy

Naval Ordnance Station
Technical Library
Indian Head, MD 20640 — 1 copy

Naval Postgraduate School
Technical Library (Code 0212)
Monterey, CA 93940 — 1 copy

Naval Missile Center
Technical Library (Code 5632.2)
Point Mugo, CA 93010 — 1 copy

Naval Ordnance Station
Technical Library
Louisville, KY 40214 — 1 copy

Commanding Officer
Naval Ocean Research & Development Activity
NSTL Station, MS 39529 — 1 copy

Naval Surface Weapons Center
Technical Library
Silver Spring, MD 20910 — 1 copy

Naval Ship Research & Development Center
Central Library (Codes L42 and L43)
Bethesda, MD 20084 — 1 copy

Naval Avionics Facility
Technical Library
Indianpolis, IN 46218 — 1 copy

Naval Oceans Systems Center
Technical Library
San Diego, CA 92152 — 1 copy

SUPPLEMENTAL DISTRIBUTION (1 copy each)

Professor Henry Bass
Department of Physics and Astronomy
University of Mississippi
University, MS 38677

Dr. David Blackstock
Applied Research Laboratories
University of Texas
P.O. Box 8029
Austin, TX 78713-8029

Mr. Franklin Breckenridge
National Bureau of Standards
Gaithersburg, MD 20899

Professor Lawrence Cram
National Center for Physical Acoustics
P.O. Box 847
University, MS 38677

Professor Steven Garrett
Department of Physics - Code 61Gx
Naval Postgraduate School
Monterey, CA 93943-5000

Professor Robert Green
Materials Science and Engineering
The Johns Hopkins University
Baltimore, MD 21218

Professor Mark Hamilton
Department of Mechanical Engineering
University of Texas
Austin, TX 78712-1063

Professor Moises Levy
Department of Physics
The University of Wisconsin-Milwaukee
Milwaukee, WI 53201

Professor Walter Meyer
Department of Physics
Georgetown University
Washington, D.C. 20057

Professor Julian Maynard
Department of Physics
Pennsylvania State University
University Park, PA 16802

Professor Wolfgang Sachse
Theoretical and Applied Mechanics
Cornell University
Ithaca, NY 14853-1503

Professor James Wagner
Materials Science and Engineering
The Johns Hopkins University
Baltimore, MD 21218

Professor Robert Apfel
Yale University
P.O. Box 2159
New Haven, CT 06520

Dr. Roger Hackman
Code 4120
Naval Coastal Systems Center
Panama City, FL 32407-5000

Dr. W. P. Arnott
National Center for Physical Acoustics
P.O. Box 847
University, MS 38677

Dr. Kevin Williams
Applied Physics Laboratory
University of Washington
Seattle, WA 98195

Professor Calvin Quate
Department of Applied Physics
Stanford University
Stanford, CA 94305

Professor Anthony Atchley
Department of Physics - Code 61AY
Naval Postgraduate School
Monterey, CA 93943-5000

Prof. O. B. Felsen
Dept. of Electrical Engineering
Polytechnic Institute of New York
Route 110
Farmingdale, NY 11570

Dr. Robert N. Thurston
Bell Communications Research
Guided Wave and Optoelectronics
331 Newman Springs Road
Red Bank, NJ 07701